Centre for Geo-Information

Thesis Report GIRS-2006-17

ESTIMATION OF THE SPATIAL FREQUENCY DISTRIBUTION OF BIOMASS IN RIVER FLOODPLAINS

A case study using field and airborne Imaging Spectrometer data in the Millingerwaard.

MD Suarez Barranco

April / 2006

WAGENINGEN UNIVERSITY
WAGENINGEN UR

ESTIMATION OF THE SPATIAL FREQUENCY DISTRIBUTION OF BIOMASS IN RIVER FLOODPLAINS

A case study using field and Imaging Spectroscopy data in Millingerwaard

MD Suarez Barranco

Registration number 81 06 12 817 040

Supervisors:

Dr. ir. Lammert Kooistra
Prof. Dr. sc. nat. Michael E. Schaepman

A thesis submitted in partial fulfilment of the degree of Master of Science at Wageningen University and Research Centre, The Netherlands.

April, 2006

Wageningen, The Netherlands

Thesis code number: GRS-80436
Wageningen University and Research Centre
Laboratory of Geo-Information Science and Remote Sensing
Thesis Report: GIRS-2006-17

"Only If We

Can Understand

Can We Care,

Only If We Care

Will We Help,

Only If We Help

Shall All Be Saved"

(Jane Goodall)

“Sólo si podemos entender
nos puede importar,
sólo si nos importa
ayudaremos,
solo si ayudamos
podremos salvarnos”

(Jane Goodall)

ACKNOWLEDGEMENTS

I would like to thank all the people that have contributed to this thesis.

The first persons I would like to thank are my supervisors: Lammert Kooistra and Michael Schaepman. They encouraged and made scientific my way with support and advices. Sometimes even making me think I had good ideas.

I also would like to thank the people from the department of Geo-Information Sciences that when needed offered some minutes of their time to assist me.

Partners (and friends) from the master (Javi, Ana, Maria, Philipp, Silvia, Monica…and many many others) made my life easy sharing not only courses and lectures but also our living in Wageningen. I cannot forget Elisa, who helped me a lot from The Netherlands and from Spain. Rogier and Dieter helped me with my English or with smart tips. They, together with other friends like "Los bajos de Dijkgraaf" have been my family these years and made me "disconnect" sometimes and come back to reality.

My friends from Spain have always been there, even when I did not have time to call or write them. I promise they will have a reward for all this time.

Last but not least, I would like to thank my family. Without them, nothing would have been possible.

ABSTRACT

River floodplains are heterogeneous areas with high biodiversity and natural value. Nevertheless, they are constrained by river management. Biomass mapping is needed for ecological monitoring as well as input for the river management to assess hydraulic resistance of the vegetation in case of flooding.

This case study is aiming at assessing the possibilities of biomass mapping in a river floodplain using imaging spectroscopy. To achieve that, statistical methods using vegetation indices and radiative transfer modelling inversion (PROSPECT/SAIL coupled model) were used.

Due to the heterogeneity of the area the methodology applied is plant functional type-dependent. Statistical approaches can give satisfactory results but do not give globally applicable expressions. The biomass best-correlated indices were the Soil Adjusted Vegetation Index (SAVI) and the Weighted Difference Vegetation Index (WDVI).

Radiative transfer modelling on the other hand can be up-scaled or applied in other areas. The inversion of the PROSPECT/SAIL model was carried out by means of look-up-tables. The results were satisfactory in herbaceous dominated vegetation areas accounting for four species assumed to be present.

TABLE OF CONTENT

LIST OF FIGURES

LIST OF TABLES

1 INTRODUCTION

1.1 BACKGROUND

The management of landscapes requires knowledge and understanding of their characteristics e.g. biomass quantity. Productivity, species richness and biodiversity are valuable input for monitoring of changes by nature managers (Cramer, 1999). Therefore, vegetation biomass is an indicator of environmental conditions and should be well recognised and mapped. For this purpose, models predicting biomass have been developed as a method to retrieve biomass estimates from field or remotely sensed data. Biomass models (e.g. Biome3, Global Production Efficiency Model (GLO PEM), Simulateur mulTIdisciplinaire pour le Cultures Standard (STICS)) are tools to estimate vegetation biomass. They aim not only at the knowledge about carbon cycle fluxes (Cramer, 1999); to assure their preservation in time natural areas or reserves also require monitoring in which these models can assist. Moreover, the biomass frequency distribution can be used as input for modelling issues dependent on vegetation in river flood models (Trémolieres *et al.*, 1998).

There are different methods for estimating biomass. In general, we can classify them as using traditional destructive methods, such as "*cuts and weights*" (Paruelo *et al.*, 2000; Di Bella, 2004), "*double sampling methods*", developed from visual or digital image estimations (Paruelo *et al.*, 2000) and "*crop simulation models*" (Di Bella, 2004).

Biomass cut constitute a simple method to estimate biomass production (e.g. Sims *et al*., 1978; Sala *et al*., 1988) but this technique is limited by its slowness, cost and especially by the number of necessary measurements to produce reliable information (Di Bella, 2004).

"Double sample methods" or "Statistical approaches" involve the development of regression equations between biomass and variables easy to measure (Paruelo *et al.*, 2000).

"Crop simulation models" (Kanemasu, 1990; Field *et al.*, 1995) have now gained broad acceptance for translating ecological hypotheses, derived from local

observations, into estimates of regional, continental or even global outcomes of ecosystem processes (Cramer, 1999).

The last decades, Remote Sensing has offered new perspectives to complete the work in progress, taking advantage of the different spatial and temporal resolutions provided by different sensors (Prevot *et al.*, 1998). Remote Sensing is a technological tool to assess actual vegetation conditions (Hunt Jr. *et al.*, 2005). Remote Sensing provides a spatially continuous data set resulting in a continuous output; this means that additional extrapolation techniques are not needed. The number of samples is also reduced, so the sampling is not as expensive and time consuming. Furthermore, Remote Sensing permits the use of study areas on inaccessible environments (Zagajewski, 2004).

Biomass can be estimated from remote sensing data by means of statistical methods based on vegetation indices (Foody *et al.*, 2003; Zheng *et al.*, 2004; Rahman *et al.*, 2005) or by means of models that use a set of spatially continuous inputs (Ruimy *et al.*, 1999). The biomass estimation models that use remote sensing data have also been used by several authors in different field applications: in cereals (Su *et al.*, 1997; Daughtry *et al.*, 2000; Olioso *et al.*, 2002; Hunt Jr. *et al.*, 2005), in grazed-grasslands (Wylie *et al.*, 2002; Di Bella, 2004; Di Bella *et al.*, 2005), in forest (Schlerf *et al.*, 2005), and in heterogenous areas (Paruelo *et al.*, 2000; Zheng *et al.*, 2004).

In this study, imaging spectroscopy is used to achieve a biomass estimation using Radiative Transfer Models (RTM) and statistical approaches. RTM are physically based canopy reflectance models that link canopy properties with sensor-measured radiance (Liang, 2004). Since these canopy reflectance models formalize physical knowledge, they can deal, in principle, more easily with different measurement conditions (Atzberger, 2004).

In this case study imaging spectroscopy is used as input, but there are other possibilities as Light detection ranging sensors (Lidar) images that provide more information from the canopy structure and a higher spatial accuracy (Lim and Treitz, 2004).

The estimation of biomass from images obtained with Lidar yields in the correlation between laser height metrics and above-ground biomass (Drake *et al.*, 2002).

Lidar sensors send a laser pulse with a footprint size between <1 to 40 m, record x and y coordinates, and elevation within 10-15 cm. Small footprint lidar can also provide high spatial resolution data on the physical structure of the forests.

These sensors provide high-resolution data on forest height, canopy topography, vegetation volume and gap size; and provide estimates on number of strata in a forest, succession status of forest and above-ground biomass (Gillespie *et al.*, 2004).

Although the majority of the studies have been, in general, successful in estimating biomass, commonalities between reported predictor variables used in model development are rare. Consequently, studies are study- and site-specific and unable to be generalized to other vegetation types and site conditions (Lim and Treitz, 2004).

1.2 PROBLEM DESCRIPTION

Rivers in The Netherlands are kept within narrow courses demarcated by dikes and dams. This system of river management curbs the rivers' power to allow human habitation and agriculture in areas otherwise subjected to seasonal flooding (Geerling, 2005).

The river regulation measures, agriculture boom and industry establishment on the floodplains are causing loss of biodiversity. When the damages on riverside vegetation in recent years became clear, nature development projects were realized in order to compensate these losses (Geerling, 2005).

Economically speaking, both objectives about flood risk management and nature development management are important. Flood risk management projects keep the investments in the area safe. On the other hand, functional floodplains with high species diversity and habitat heterogeneity also provide economic benefits in the form of natural flood control and natural water purification (Trémolieres *et al.*, 1998). Moreover, nature values are always profitable by means of recreational activities and ecosystem services, such as food, pasture, fuel, timber and fibres, medicine and chemical production (De Groot *et al.*, 2002).

Initiatives have already started with the aim of preserving the sustainability of floodplains at the same time controlling flooding risks. One example is *Freude am Fluss* to find a solution to the "safety-versus-nature dilemma" (Web 1). In Figure 25, appendix 1, a map with the area influenced by the Freude am Fluss project can be found.

The assessment of the sustainability of floodplain rejuvenation is input for flood risk management and nature restoration strategies. Specialists state that the amount of vegetation in the river floodplains has increased in the last ten years in The Netherlands. In a non-disturbed situation, the river would regulate the amount of vegetation in a natural way by means of a cyclic rejuvenation. In regulated river systems, man-made rejuvenation is needed as natural rejuvenation is not possible in the river bed restricted by dikes (Web 2).

To make a decision about the measures and where to reduce biomass, spatial explicit information on the vegetation biomass in river floodplains in the Netherlands is needed.

In order to have a successful management on the riverside lands of the River Rhine, a good database about vegetation development of the area is needed. Not only the nature management projects but also the flooding risk managements use vegetation as input in their models as stated before in this chapter.

The approach of this study consists on retrieving the spatial distribution of the biomass values in the study area of the floodplain Millingerwaard as a case study (quantitative surface values of each biomass level). The hypothesis is that nature management is directed towards a horizontal distribution of biomass frequency. If the distribution approaches a constant horizontal line (Figure 1), all PFTs are equally represented in the area so biodiversity is preserved and the heterogeneous landscape is kept. With this approach, succession and species richness can be monitored better.

As a conclusion, the study of the biomass distribution curve could be used as input in both nature and water management approaches.

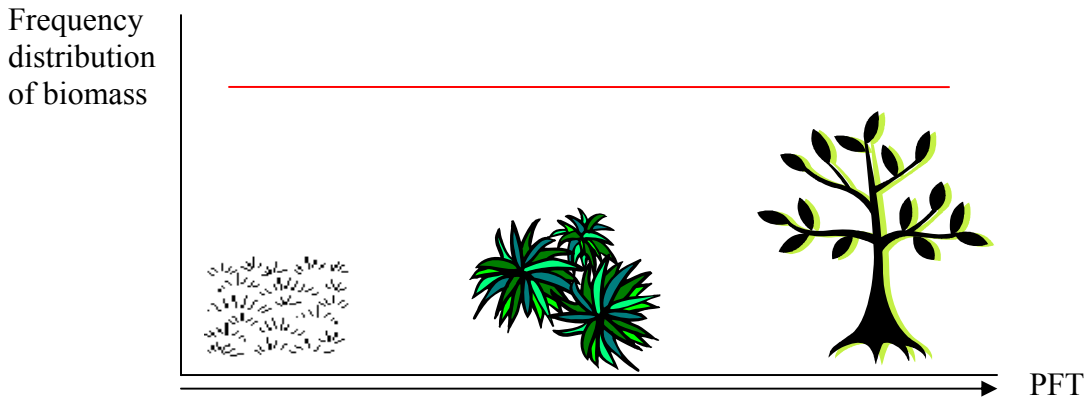

Figure 1..... Spatial frequency distribution of biomass measured in terms of PFTs.

1.3 RESEARCH OBJECTIVES

The main research objective is to *estimate the biomass frequency distribution in the floodplain Millingerwaard using remote sensing techniques*. Biomass in the scope of this research is considered as being dry weight of fresh vegetation per surface unit ($gr.cm^{-2}$). The management of this nature area can then be improved by taking into account ecological and flood prevention objectives. The Millingerwaard area is characterized by its significant heterogeneity in plant functional types (grass/herbs, shrubs and forest) and its regional scale. For this purpose, imaging spectroscopy data are available as well as other field samples that can be used for validation.

The main research question is:

- What is the actual biomass frequency distribution in the floodplain Millingerwaard?

The research sub questions can be stated as follows:

- What are the results for estimating the spatial biomass distribution with statistical models from vegetation indices?
- How can we use imaging spectroscopy for the estimation of biomass by means of the use of Radiative Transfer Models in the Millingerwaard?

The thesis work consists of: (1) Estimation of biomass ($gr.cm^{-2}$) using statistical methods from different vegetation indices derived from imaging spectroscopy data and comparison between the different estimations by means of the correlation coefficient. (2) Estimation of biomass in Millingerwaard using RTM, concretely the SAIL-PROSPECT model. (3) Validation of the results coming from the application of RTM with the biomass values from the field. (4) Plotting distribution of biomass and analysis of the results. (5) Find out some recommendations for up-scaling results to other similar areas with the possibility of using other input data as for example Landsat images.

1.4 STRUCTURE OF THE REPORT

The first introductory chapter (1. Introduction) of this report explains the background of the case study, problem definition and objectives. In the second chapter (2. Literature review) the main concepts are defined in the scope of the research. The third chapter (3. Materials and methods) consist of the description of the study area, data collection and availability and procedures applied in the research. The fourth chapter (4. Results) presents the output from the methodology of the previous chapter. Chapter 5 is a discussion of the results and the last chapter (Chapter 6. Conclusions and recommendations) explains the final conclusions and some recommendations for future research to be performed in this field.

2 LITERATURE REVIEW

2.1 DEFINITION OF BIOMASS

According to the Australian State on the Environment report, biomass is the "quantity of organic materials within an ecosystem usually expressed in dry weight per unit area or volume" (Hamblin, 2001). This term is related to the Net Primary Productivity (NPP) that is defined by the same source as being "the ratio of all biomass accumulation and biomass losses in units of carbon, weight or energy, per land/surface unit, over a set time interval" (Hamblin, 2001). Net Primary Productivity is then an important variable in the carbon cycle as it determines the rate of absorption of atmospheric carbon by land vegetation. (Ruimy *et al.*, 1999). Moreover, as NPP is calculated as a rate of biomass, estimating biomass is essential for understanding the dynamics of sources and sinks of atmospheric carbon (Rahman *et al.*, 2005).

Both, biomass and NPP are used to monitor the carbon fluxes, study productivities, nutrient allocation and fuel accumulation in terrestrial ecosystems (Zheng *et al.*, 2004).

2.2 PLANT FUNCTIONAL TYPES AND HYDRAULIC RESISTANCE

In a floodplain area like Millingerwaard, the river managers worry about the riverside natural vegetation and its influence in the discharge capacity of the river. Their management can be improved by studying the presence of the different vegetation types and their hydraulic resistance (van den Bosch, 2003). The hydraulic resistance is the magnitude of the turbulence resulting from water in laminar regime passing through an obstacle (Figure 2). Its value affects the velocity of the regime and depends on the shape and characteristics of the obstacle. Figure 3 shows examples of the hydraulic resistance values of different Plant Functional Types used by the water authority.

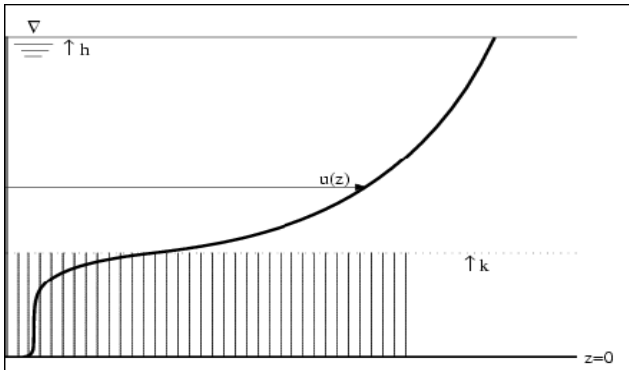

Figure 2..... Typical vertical profile of horizontal flow velocity for submerged vegetation, h is water depth; k is vegetation height (Keijzer *et al.*, 2005).

Determinant for the hydraulic resistance of the vegetation is the area of contact, which first of all depends on the water level and the height of vegetation (Figure 2). The vegetation structure plays a role through the height, diameter and density of stems, the height branches shoot, the density of branches and the surface area of leaves.

The *Nikuradse equivalent roughness* (*K)* constant is one of the possible expressions of hydraulic resistance. In Figure 3 we can see an example of the values this constant has for different plant functional types (Geerling, 2005).

Figure 3 shows that bushes have the highest hydraulic resistance of the presented plant functional types. The plant functional types are classified according to the River Ecotope System (RES) as described by Rademakers and Wolfert (Rademacher and Wolfert, 1994).

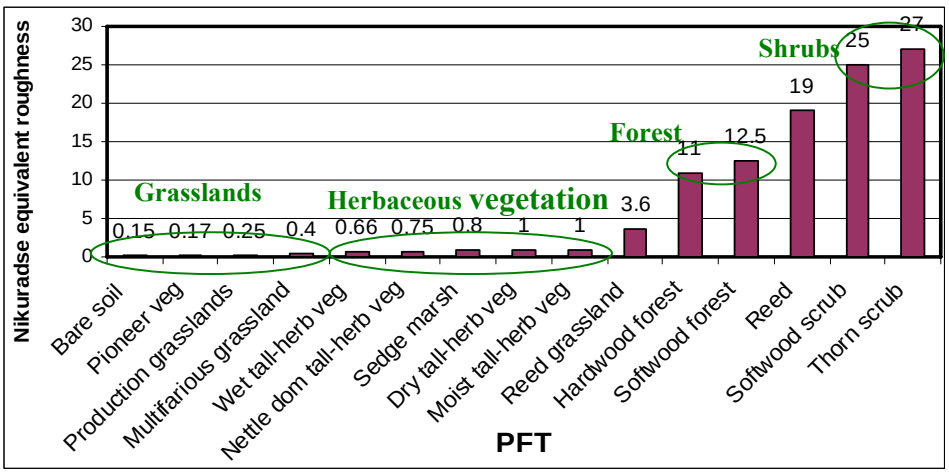

Figure 3..... Hydraulic resistance per Plant Functional Type in the river floodplain measured in terms of Nikuradse equivalent roughness (m) (Geerling, 2005).

The hydraulic resistance of shrubs is high because they have dense structure beginning at the soil level. Forest areas leave more freedom to the water as the ramification starts at a higher level. Herbaceous vegetation and grasslands are the plant functional types that are almost not obstacle for the water to run.

"Plant functional type" is a term used by several authors to define cluster of species with similar morphology and phenology (Paruelo and Lauenroth, 1996; Laurent *et al.*, 2004).

Flood risk (defined as flooding probability and potential damage) along the river Rhine is expected to increase in the coming decades. The two main reasons are (Hooijer, 2002):

- Climate change will cause a significant increase in the probability of extreme floods, and
- Increasing level of investments in areas at risk doubles every three decades. This promotes the potential damage of floods.

That is why flood risk management strategies and measures should be developed in anticipation of higher peak discharges in the future (Hooijer, 2002).

2.3 REMOTE SENSING METHODS FOR ESTIMATING BIOMASS

There are essentially three ways of estimating vegetation biomass from remote sensing data according to Cramer (1999): (1) Using Production Efficiency Models (PEMs); (2) By means of biomass-vegetation indices correlation; or (3) Using Soil-Vegetation-Atmosphere-Transfer Models (SVAT). (1) and (3) are *Crop simulation models* and (2) are *Double sampling methods* (Section 1.1 in this report).

2.3.1 PRODUCTION EFFICIENCY MODELS (PEMs)

These models are also called "diagnostic models". They are based on the Kumar & Monteith (1981) approach. The fraction of solar radiation absorbed is calculated from remote sensing data and then derived into production. They use the concept of *Light*

Use Efficiency (LUT) for the conversion of *Absorbed Photosynthetically Active Radiation* (APAR) to biomass (Cramer *et al.*, 1999).

2.3.2 STATISTICAL APPROACHES ESTIMATING BIOMASS

The statistical methods are based on correlation relationships of land surface variables with remotely sensed data. They are easy to develop and effective for summarizing local data (Liang, 2004).

The feasibility of using multispectral reflectance data for estimating dry vegetation biomass production was addressed by (Aase and Siddoway, 1981) who developed regression equations between canopy spectral reflectance and total dry vegetation biomass of wheat.

Recent literature has shown that the narrow bands may be crucial for providing additional information with significant improvements over broad bands in quantifying biophysical characteristics of vegetation (Thenkabail *et al.*, 2000).

In local estimations, the use of empirical-statistical approaches can give satisfactory results (Aztberger *et al*, 2003; Prince and Bausch, 1995). However, since canopy reflectance depends on a number of factors, no unique relationship between the spectral signature and the canopy variables can be expected to be applicable everywhere and all the time, even for a particular sensor. Consequently, empirical-statistical relationships are highly site- and sensor-specific and unsuitable for large areas or in different seasons. (e.g., Curran, 1994; Gobron et al., 1997).

There are previous studies that have applied statistical approaches to estimate biomass in grasslands and forest. In tables 1 and 2 some of them are showed.

Table 1. Literature review of biomass estimations from vegetation indices with different sensors for grasslands

Vegetation Index	**Sensor**	**R^2**	**Source**
NDVI	Hypersp. 1m	0.39	(Mirik *et al.*, 2005)
	Landsat TM	0.95, 0.81	(Wylie *et al.*, 2002; Reeves *et al.*, 2006)
	ASTER	0.82	(Reeves *et al.*, 2006)
SRTVI	Hypersp. 1m	0.39	(Mirik *et al.*, 2005)

Table 2. Literature review about biomass estimations of vegetation indices with different sensors for forest

Vegetation Index	Sensor	R^2	Source
NDVI	Hypersp. 1m	0.66	(Mirik *et al.*, 2005)
	Landsat TM	0.82	(Rahman *et al.*, 2005)
SRTVI	Hypersp. 1m	0.66	(Mirik *et al.*, 2005)
	Landsat TM	0.82	(Zheng *et al.*, 2004)
SAVI	Landsat TM	0.046	(Rahman *et al.*, 2005)
TVI	Landsat TM	0.229	(Rahman *et al.*, 2005)

In grasslands only NDVI and SRTVI have been applied. Good correlation coefficients were obtained when correlating NDVI derived from Landsat and Aster with biomass.

In the last years indices related with the water content in the leaves have been created (Ceccato *et al.*, 2002). These indices minimise perturbing geophysical and atmospheric effects. The relationship of those indices with the dry matter on the one hand and the wet matter on the other hand can be a further study.

Although local statistical estimations can not be applied directly to other areas, local methods can be up-scaled and extrapolated. In this case study, statistically based estimations are done to complete results from radiative transfer models.

2.3.3 RADIATIVE TRANSFER MODELS

Radiative Transfer models are physically based canopy reflectance models that link canopy properties with sensor-measured radiance (Liang, 2004). At the top of the canopy, the interaction of radiation within the vegetation depends on the contribution of several components such as leaves, stems, soil background as well as the illumination and view geometries. Canopy reflectance will thus depend on the optical properties of each canopy element, as well as on their number, area, orientation, and position in space (Goel and Thompson, 2000; Koetz *et al.*, 2005).

The PROSPECT model (Jacquemoud and Baret, 1990) is used to describe leaf optical properties (Figure 4). PROSPECT simulates leaf reflectance and transmittance spectra as a function of leaf biochemical contents and leaf structure.

The input parameters for the PROSPECT model are a structure parameter (N), Chlorophyll a and b content C_{ab} (µg./cm^2), Equivalent water thickness C_w (cm), dry matter content in the leaves C_m (g./cm^2) and brown pigment concentration in the leaves C_b. The output is an ASCII file with the modelled reflectance and transmittance in the leaves of the canopy.

Jacquemoud and Baret (1990) concluded after the creation of PROSPECT model that there are uncertainties in it. Those uncertainties come from the assumptions made. It is assumed the uniformity in the distribution of water, pigments and structure inside the leaf. The absorption coefficient is influenced by the difficulty of discriminating between different pigments inside the leaf. And finally, the angle which represents the surface roughness was supposed to be constant(Jacquemoud *et al.*, 1995).

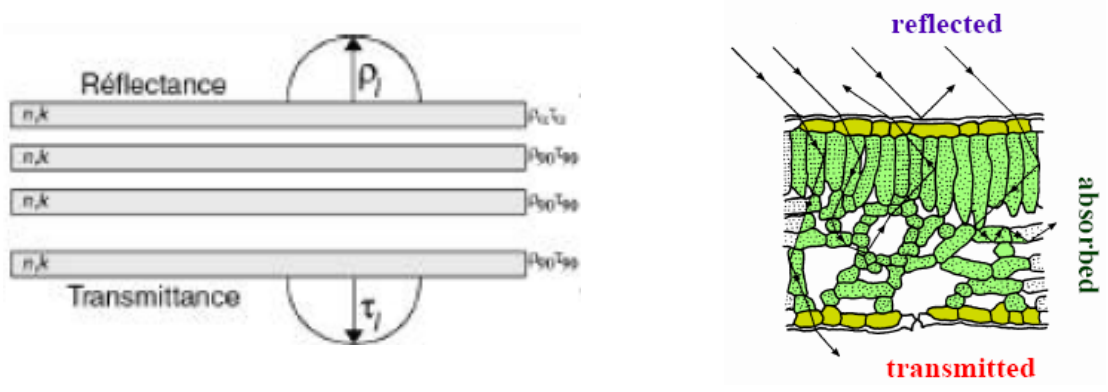

Figure 4..... Schematic representation of Prospect model. The leaf is represented as a pile of absorbing plates with rough surfaces.

An often used model for simulating canopy reflectance is the SAIL model (Scattering from Arbitrarily Inclined Leaves) (Verhoef, 1984). It describes the canopy structure in a fairly simple way while producing nevertheless realistic results as reported by several authors for different crops. Goel and Thompson (1984) studied the difference between planophyle and erectophile crops and independently in soybean; Jacquemoud in 1995 in sugar beet (Jacquemoud *et al.*, 1995) and in 2000 in soybean and corn (Jacquemoud *et al.*, 2000).

The input parameters for SAIL model are the Leaf Area Index (*LAI*), Average Leaf Angle (*ALA*) (degrees), hot spot parameter, view zenith angle (radians), sun zenith angle (radians), diffuse fraction, soil background spectra (%) and leaf spectra (%).

A combination of the two models described above is available, namely SAIL/PROSPECT Radiative Transfer Model (Figure 5). The coupled model SAIL/PROSPECT use the PROSPECT leaf reflectance output as input in the SAIL model to estimate the total canopy reflectance.

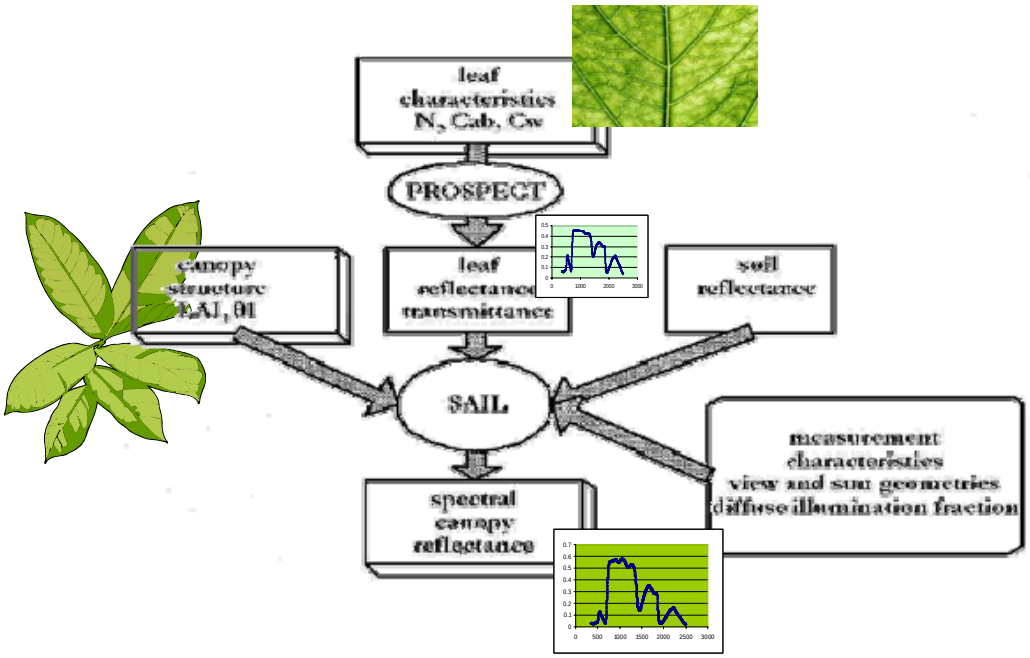

Figure 5..... Coupled SAIL/PROSPECT radiative transfer model for plant canopies. The entire wavelength range (400mm-2500mm) is modelled using only a few parameters (Jacquemoud, 1993).

Model inversion

When Jacquemoud and Baret (1990) created the Prospect model, they gave already the idea of using it in combination with canopy reflectance models. Moreover, they also suggested the possibility of inverting the model to get biophysical variables from the canopy in a non-destructive way.

Nevertheless, the model inversion does not assure a certain quality retrieval of parameters. There are two main reasons according to Atzberger (2004) why the inversion of canopy reflectance models is an ill-posed problem:

- Different model parameterization may yield almost identical spectra.
- There are uncertainties in the model and in the reflectance measurements (e.g. assumptions in the model and sensor noise in the reflectance data collection).

According to Goel and Thompson (1984), two conditions are necessary for estimating canopy variables from spectral signatures of vegetation: an accurate model and the choice of an appropriate inversion procedure.

There are three main techniques to invert physically based models. Iterative methods require long computational time (Liang, 2004) while Look-up-tables and Artificial Neural Network are not inherently designed to be easily generalized to any view-sun configurations (Gastellu-Etchegorry *et al.*, 2003).

In this case study the inversion was done by means of look-up-tables. The look-up-table is one of the simplest techniques used to invert models (Weiss *et al.*, 2000). This technique consists of generating a table "$m \times n$" where "m" is the number of combinations of input variables simulated with the model and "n" is the number of bands extracted from the simulated spectra. In the application phase, for a given reflectance measurements in the n bands, the elements of the reflectance that are the closest to the measurement are selected, and the corresponding set of input variables in the table represents the solution of the problem.

In this study, the distance criterion that corresponds to the cost function in optimization techniques was defined as the relative root mean square error (*RMSE*) between the measured reflectance r and the estimated reflectance r' found in the look-up-table (Weiss *et al.*, 2000).

$$RMSE = \sqrt{\left(\frac{\sum (r - r')^2}{n}\right)}$$

Where:

r= Measured reflectance

r'= Simulated reflectance

n= number of considered bands in the look-up-table

The heterogeneity of the study area adds a difficulty to the accuracy of the model inversion. The look-up-tables are created for fixed values of the input parameters, so each pixel in which the inversion is carried out is considered homogeneous. Different look-up-tables can be created based on different species but still it is assumed that only one species is present per pixel.

There are studies done on heterogeneous areas in which a detailed sub-pixel technique is applied in the inversion procedure (Weiss *et al.*, 2000). This was achieved by dividing the data sets in three subsets corresponding to low, medium and high values of the biophysical variable considered. The reflectance and corresponding biophysical variables of these three subsets were linearly combined to simulate a larger range of heterogeneity for the mixed pixels.

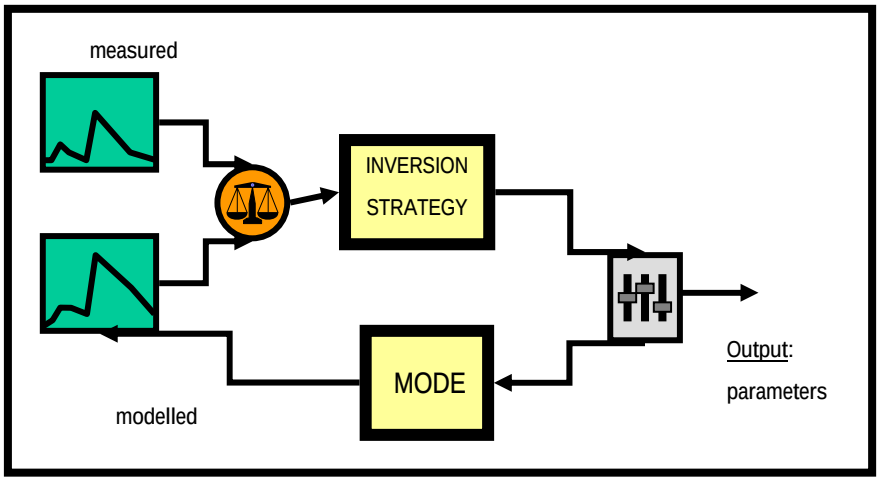

Figure 6..... Overview of the general model inversion procedure (Verhoef and Bach, 2003).

2.4 THE USE OF LANDSAT IMAGES ESTIMATING BIOMASS

Mapping of continuous biophysical variables from high-resolution imaginary such as Landsat Thematic Mapper (TM) or Enhanced Thematic Mapper Plus (ETM+) has largely depended on modelling empirical relationships derived from vegetation indices (Cohen *et al.*, 2003). Table 3 gives an overview of the different Landsat bands and their relevant characteristics.

Although Landsat multi-spectral information can provide useful indices to estimate biophysical variables, relationships for one site may not be applied at other sites due to variation in range and soil conditions (Merrill *et al.*, 1993).

The approach of estimating biomass using Landsat TM images has been carried out by different authors for grasslands (Merrill *et al.*, 1993; Todd *et al.*, 1998; Schino *et al.*, 2003; Samimi and Kraus, 2004), in crop areas (Lobell *et al.*, 2003; Thenkabail, 2003; Calvao and Palmeirim, 2004), in forest (Lu, 2005) and in heterogeneous natural areas (Shoshany, 2000). All the authors cited before used statistical methods based on biomass correlations with band combinations.

Table 3. Landsat bands spectral range, EM regions, and applications details.

Band Number	**Spectral Range (in Microns)**	**EM Region**	**Generalised Application Details**
1	0.45 - 0.52	Visible Blue	Coastal water mapping, differentiation of vegetation from soils
2	0.52 - 0.60	Visible Green	Assessment of vegetation vigour
3	0.63 - 0.69	Visible Red	Chlorophyll absorption for vegetation differentiation
4	0.76 - 0.90	Near Infrared	Biomass surveys and delineation of water bodies
5	1.55 - 1.75	Middle Infrared	Vegetation and soil moisture measurements; differentiation between snow and cloud
6	10.40- 12.50	Thermal Infrared	Thermal mapping, soil moisture studies and plant heat stress measurement
7	2.08 - 2.35	Middle Infrared	Hydrothermal mapping

In the case of grasslands areas, the best biomass-correlated indices derived from Landsat were ratios combining bands 1, 2, 5 and 7 (Samimi and Kraus, 2004). In forest areas bands 4, 5 and 7 were used to be individually correlated with biomass samples from the field (Lu, 2005). In natural areas with vegetation species heterogeneity, first a classification in PFTs is recommended (Shoshany, 2000). In a next step biomass can be estimated for each PFT. Table 4 gives an overview of the vegetation indices and Landsat TM bands used to estimate biomass in previous studies.

About the PFT classification, there are different ideas from previous studies. Grignetti (1997) concluded that the most suitable Landsat bands to use as input in a PFTs classification were bands 3, 4, 5 and 7 (Grignetti *et al.*, 1997). Smith (1990) recommended the utilization of unmixing techniques in heterogeneous areas with low spatial resolution sensors as Landsat (Smith *et al.*, 1990).

Table 4. Vegetation indices (VI) and bands used to estimate biomass by statistical approaches with Landsat images, vegetation type, correlation coefficient, kind of relation and source.

VI	**Vegetation type**	**r^2**	**Source**	**Relation**
NDVI	Grasslands	0.95	(Wylie *et al.*, 2002)	Linear
		0.81	(Reeves *et al.*, 2006)	Linear
	Forest	0.128	(Mallinis *et al.*, 2004)	Linear
		0.82	(Rahman *et al.*, 2005)	Linear
	Forest (pine)	0.86	(Zheng *et al.*, 2004)	Sigmoidal
SAVI	Forest	0.046	(Rahman *et al.*, 2005)	Linear
TVI	Forest	0.229	(Rahman *et al.*, 2005)	Linear
TM Bands	**Vegetation type**	**r^2**	**Source**	**Relation**
TM2/TM1	Grasslands	0.83	(Samimi and Kraus, 2004)	2nd order
TM7/TM1		0.79	(Samimi and Kraus, 2004)	2nd order
TM2xTM5/TM3		0.76	(Samimi and Kraus, 2004)	2nd order
TM2/TM1	Heterogeneous	0.81	(Samimi and Kraus, 2004)	2nd order
TM7/TM1		0.75	(Samimi and Kraus, 2004)	2nd order
TM2xTM5/TM3		0.76	(Samimi and Kraus, 2004)	2nd order
TM1, TM7	Forest	0.35	(Mallinis *et al.*, 2004)	Linear
TM2, TM3, TM7		0.309	(Mallinis *et al.*, 2004)	Linear
TM2, TM3, TM5, TM7		0.334	(Mallinis *et al.*, 2004)	Linear

3 MATERIALS AND METHODS

3.1 INTRODUCTION

The general procedure of this case study can be divided into two main parts. Both of them are methods to estimate biomass from remote sensing data.

The first approach uses statistics as basis. Figure 7 summarizes the statistical procedure carried out.

From the Hymap image, the vegetation indices are derived. Then, the vegetation indices are compared in the sample locations with the biomass values from the field. Finally, the biomass map is prepared using the best VI-Biomass relationships applied per plant functional types.

In the second approach the PROSPECT/SAIL coupled model is used, in Figure 8 the steps are presented. The PROSPECT/SAIL inversion to estimate biomass was carried out using look-up-tables (LUT). These look-up-tables are built with outputs of the model simulations.

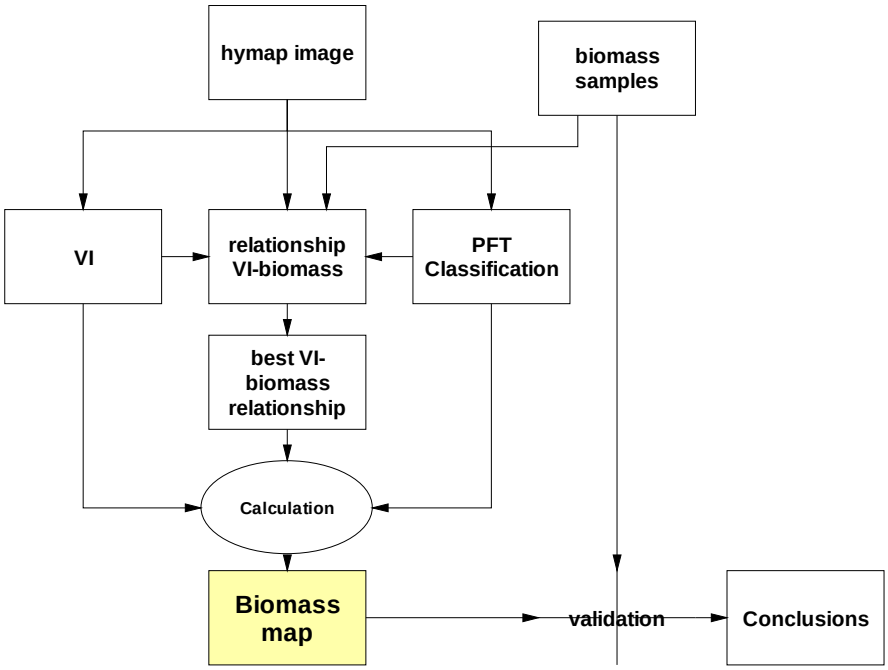

Figure 7..... Flowchart of the Statistical approach for estimating vegetation biomass from vegetation indices derived from a Hymap image.

From the inversion, leaf area index (LAI) and dry matter content in the leaves (Cm) are obtained as output. The estimated dry biomass of the canopy leaves is calculated multiplying LAI and Cm.

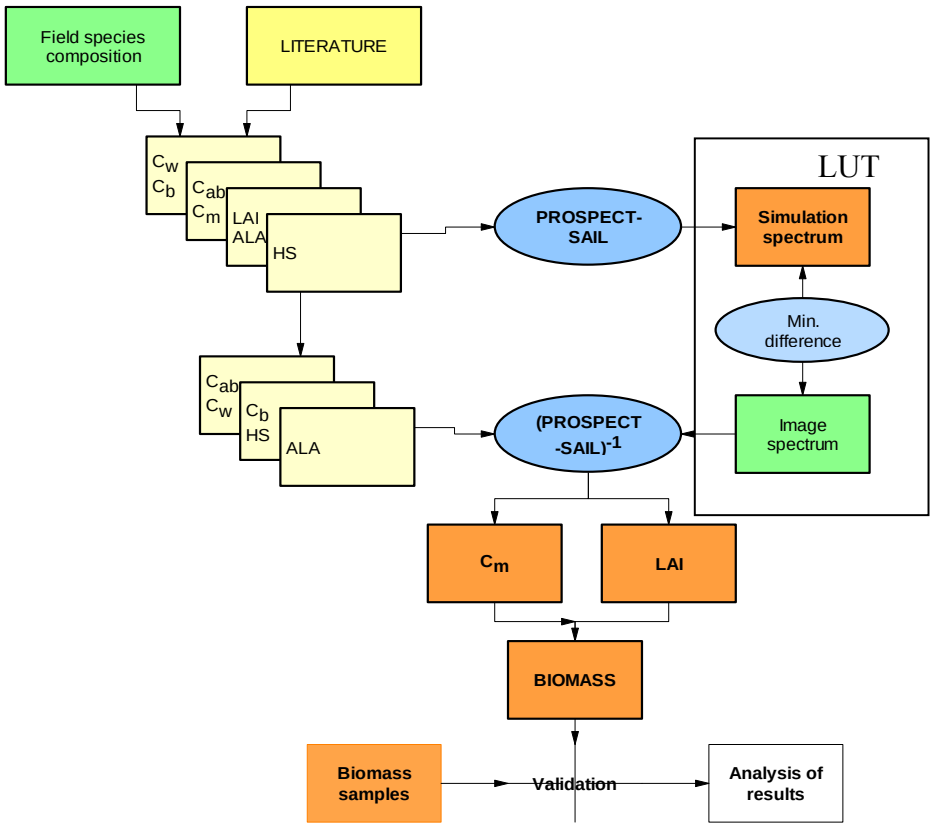

Figure 8..... Flowchart of the Radiative Transfer Models approach for estimating vegetation biomass from remotely sensed data.

3.2 STUDY AREA

The floodplain Millingerwaard is located to the east of Nijmegen along one branch of the river Rhine. It belongs to the natural reserve Gelderse Poort, a large floodplain area of 1200 ha along the river Rhine, close to the Dutch-German border. This location belongs to the nature-safety dilemma research area along the Rhine River (in the appendix 1 (Figure 25) a map of the area affected by the project *Freude am Fluss* is included). In *Freude am Fluss*, a total of eleven authorities, research institutions, and companies in three countries: the Netherlands, Germany, and France participate. An integral management plan for the area was published in 2000 under the lead of the Ministry of Transport, Public Works and Water Management. This planning included developing river related nature (SDF, 2003).

Nature rehabilitation means that step by step, individual floodplains are taken out of agricultural production and are allowed to undergo their natural succession. This has resulted for the Millingerwaard in a heterogeneous landscape with river dunes along the river, a large softwood forest in the eastern part along the winter dike and in the intermediate area in a mosaic pattern of different succession stages (pioneer, grassland, shrubs). In addition, several man-made lakes, e.g., old clay pits, are present. Nature management (e.g., grazing) within the floodplain is aiming at improvement of the typical biodiversity of the floodplains. However, the discharge capacity of the river should be above the critical safety levels during flooding events (Kooistra, 2005).

The vegetation in the area can be divided into four main Plant Functional Types (PFT) in the scope of this study: “Grazed Grasslands”, “Mixed Herbs”, “Shrubs” and “Forest”. This division is made according to their canopy height and structure. A more elaborate explanation of the PFT classification of the study area is given in section 3.5.2 of the report.

3.3 AIRBORNE IMAGING SPECTROSCOPY DATA

Imaging spectroscopy data for the Millingerwaard were acquired on the 28th of July and the 2nd of August of 2004 with the Hymap instrument (Kooistra, 2005). An overview of the complete Image Spectroscopy acquisition can be seen in Table 5.

The presented results in this paper are based on the first flight line for HyMap acquisition on 28th of July 2004. A complete spectrum over the range of 450-2480 nm is recorded with a bandwidth of 15-20 nm by 4 spectrographic modules. Each module provides 32 spectral channels giving a total of 128 spectral measurements for each pixel. However, the delivered data contains 126 bands because the first and last band of the first spectrometer is deleted during pre-processing. Ground resolution of the images is 5 m (Kooistra, 2005).

Table 5. Overview of the Image Spectroscopy campaign in Millingerwaard

Image spectrometry	**HyMap (5 m)**	**2 flight-lines**		**Specifications**
Acquisition time		28/7 13:30	2/8 10:30	126 bands
Quality flight line 1		Okay	cloud cover (not used)	450-2480 nm
Quality flight line 2		cloud cover (partly used)	okay	bandwidth 15-20 nm

Table 6. Overview of the operational equipment during the two Hymap image acquisition dates of 28th of July and 2nd of August 2004 in the Millingerwaard.

	Instrument	**#Locations**	**Date**	**Variables**
atmospheric conditions	Sunphotometer	1	2/8 2004	aerosol optical thickness
radiometric correction	Fieldspec FR	19 (5x5 m)	28/7 and 2/8 2004	VNIR spectra (sand, clay, asphalt, water)
radiometric vegetation	Fieldspec FR	21 (5x5 m)	28/7 2004	top-of-canopy and leaf spectra (VNIR)
canopy structure	hemispherical camera	13 (20x20 m)	28/7 – 6/8 2004	LAI, gap fraction, leaf angle distribution
vegetation description	Braun-Blanquet method	21 (2x2 m)	13-16/8 2004	structure, species composition
sampling vegetation	laboratory analysis	21 (0.5x0.5 m)	13-16/8 2004	biomass, N and P concentration
surface characteristics	theta probe, temperature gun	86	28/7 2004	soil moisture and temperature

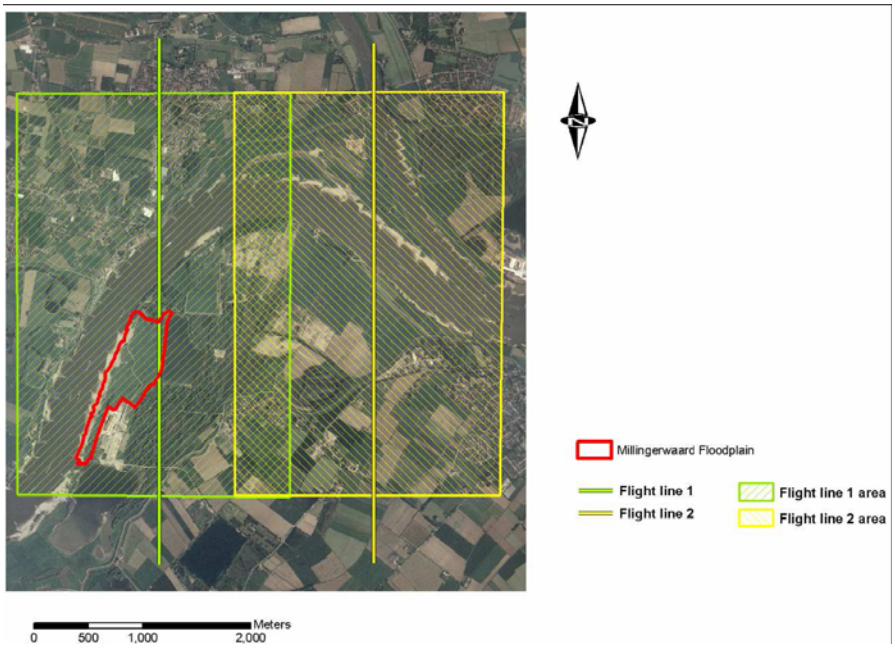

Figure 9..... Overview of the total area acquired with the Hymap instrument, Millingerwaard in the line 1.

The flight line was oriented close to the solar principal plane to minimize directional effects. The Hymap images were geo-atmospherically processed to obtain geo-coded top-of-canopy reflectance data. Visibility was estimated by combining sun photometer measurements (Table 6) with Modtran4 radiative transfer simulation.

Visibility during the flight of 2nd of August was 15 km. An image quality assessment revealed that 9 of the 126 bands should be used with caution, due to significant spatial noise (Kooistra, 2005). Not the whole acquired image was used in this study. A masking operation was carried out to select the vegetated areas. As in previous studies in the area (Kooistra, 2005), pure vegetation pixels selection was done by applying a mask based on a NDVI minimum threshold of 0.2 and a maximum reflectance at the wavelength of 665 nm (Band 13) of 7.4%. These procedures were carried out in ENVI software before applying further analysis techniques to the image.

3.4 FIELD DATA

In the field campaign, the members of the "HyEco'04" project team took ground measurements. The 21 sampling locations (Figure 10) were selected based on an available vegetation map of the study area (2002) and a preliminary survey. In each location, a plot 2 x 2 meters was selected with a relatively homogeneous vegetation cover. Three biomass samples of subplots measuring 0.5 x 0.5 m were taken per plot at 0.5 cm above the ground level. The collected material was stored in paper bags; air-dried, first for 5 days at room temperature in open bags, and subsequently for 24 h at 70ºC, and weighed to obtain the dry biomass (g).

Dry biomass values of each subplot were stored in weight/area units. The dry biomass per plot was calculated by means of the average between the dry biomass of the corresponding subplots. Final values are expressed in gr/m^2 units.

Table 20 is showing the most dominant specie in each sampling plot, its coverage percentage and the average height. From this information the PFT is defined. The plots where this information is missing are classified according to the pictures taken in the field campaign.

In the two-week period after the image acquisition, vegetation descriptions were made for the 21 locations according to the method of Braun-Blanquet (Braun-Blanquet, 1951). Abundance per species was estimated optically as percentage soil covered by living biomass in vertical projection, and scored in a nine-point scale.

Table 7. Statistical values of the field samples ($gr.cm^{-2}$)

	All	Grazed-grasslands	Mixed-herbs
Mean	516.823	304.143	623.163
Standard Error	55.84	69.08	59.032
Median	572.44	258.68	634.58
Standard Deviation	255.891	182.769	220.878
Sample Variance	65480.168	33404.368	48787.15
Range	1037.32	445.12	922.76
Minimum	127.32	127.32	241.88
Maximum	1164.64	572.44	1164.64
Sum	10853.28	2129	8724.28
Count	21	7	14

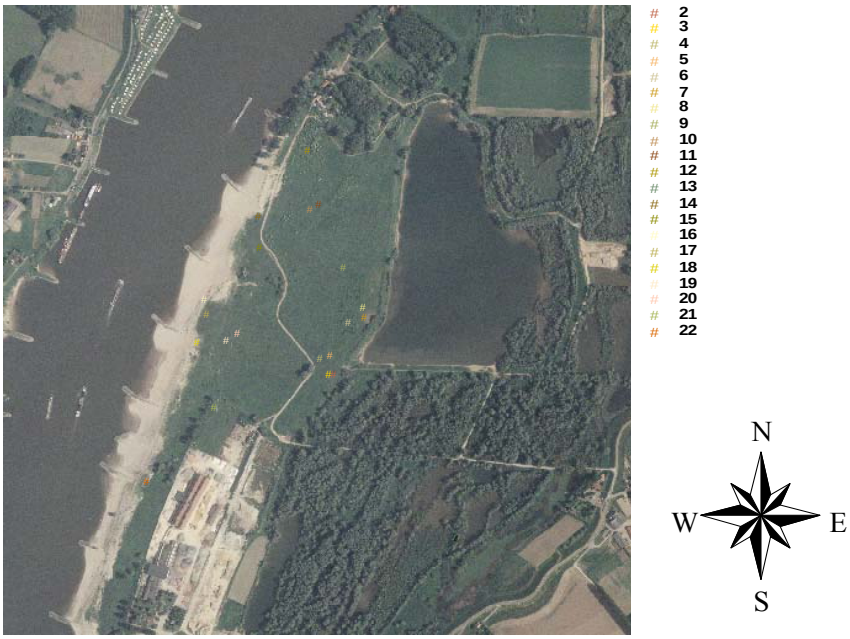

Figure 10. .. Sampling locations in the campaign HyEco'04. The biomass samples correspond to the vegetation sample points.

A description of the vegetation was made for the 21 plots (2 x 2 m) that were also radiometrically characterized. Locations of the plots are shown in Figure 10. The vegetation descriptions were made according to the method of Braun-Blanquet (1951).

3.5 PLANT FUNCTIONAL TYPES

3.5.1 Definition

As there were not biomass samples in forested neither shrubs areas, the samples were then divided in two main plant functional types: Grazed-Grassland (7 samples) and Mixed-herbaceous (14 samples) where herbaceous species are present and only one shrub species dominates some samples, namely *Rubus caesius*. In figure 10 the sampling points in the field campaign are represented.

The division in PFT was based on the vegetation description that was made during the field work (section 3.4). The parameters used for the classification were "height of the crop" "management" and "species composition". The intervals considered for herbs and shrubs respectively were the ones in Table 8.

Table 8. Height ranges considered in the division in PFT in the study for the division, the parameters ¨height ranges¨ and "dominant species" were taken into account.

Height ranges (cm)			**Management**	**Dominant species**
PFT	**Minimum**	**Maximum**		
Grazed-Grasslands	0	40	Grazing	*Trifolium repens, Potentilla reptans, Cynodon dactylon*
Mixed-Herbs	40	120	No	*Rubus caesius, Calamagrostis epigejos, Urtica dioica*

Table 9. Percentage of proportional coverage of Trifolium repens, Calamagrostis epigejos, Urtica dioica and Rubus caesius in the 2 PFT sampling plot groups.

	Grazed-grasslands	**Mixed-herbs**
Trifolium repens	25.71%	0%
Urtica dioica	0.57%	6.57%
Calamagrostis epigejos	2.14%	16%
Rubus caesius	0%	34.93%

Figure 11. .. Example of the two main PFT in Millingerwaard. In the picture of the left, plot number 2 belonging to the Grazed-Grasslands plant functional type, on the right, plot number 12 from Mixed-herbs plant functional type.

Then, the samples without height information were included in one group or the other based on information from photographs taken during the field work. In the pictures in Figure 11, there is one example of each plant functional type.

Moreover, managed and non-managed plots were also separated to get a more accurate relationship between biomass and the different vegetation indices. The management can influence the age of the vegetation. In this case, the managed areas corresponded to the samples considered Grazed-grassland.

3.5.2 Classification using Mixture Tuned Match Filtering

After a classification of the samples in plant functional types, a classification map of the area was done. The difficulties of getting a good classification were the high heterogeneity of the area and the high number of species per PFT. Then, to find the technique that better fits the research area, two classification methods were tested: Linear Spectral Unmixing and Mixture Tuned Match Filtering (Boardman, 1998). Moreover, to simplify the image and avoid noisy spectral bands, a selection of eight bands was done and the classification process was carried out again.

Summing up, two classification methods were used with the whole spectrum and with a selection of 8 bands. The resulting maps were analyzed with the knowledge about the area and checked in the sample points.

The Mixture Tuned Matched Filtering (MTMF) method was chosen to make the classification of the Millingerwaard in PFT because other authors (Williams and Hunt Jr., 2002; Mundt *et al.*, 2005) had used this classification method in previous studies in areas with a relatively high vegetation heterogeneity (e.g. prairie sites mixed with woody areas). The classification procedures were carried out in ENVI software.

The MTMF is based on a previous transformation known as Maximum Noise Fraction (MNF) which was defined to be as a substitute of Principal Component Analysis (PCA) transformation (Green *et al.*, 1988). This tool is a method for ordering components in terms of image quality and was created based on the poor performance of the PCA for example with *ATM simulator* data. MNF is identical with the standard principal components transformation when the noise variances in all bands are equal. When noise is in one band only, multiple linear regression is applied so this band is not taken into account (Green *et al.*, 1988).

MTMF is a partial unmixing algorithm that is capable of determining target abundance within a pixel (Boardman, 1998). It has in common with the Linear Spectral Unmixing (LSU) the constraints about the sum of the classes per pixel equal to 1 and the use of values between 0 and 1. Moreover, none of the two methods in ENVI software can be fully constrained applied. On the other hand, using MTMF, information about all the present end-members spectra is not needed, what makes

MTMF different from LSU and more similar to Matched Filtered models (Boardman, 1998).

The selection of the spectral bands was done, in the case of the Linear Spectral Unmixing Classification, based on the representative bands of the spectra of the endmembers (table 10 and Figure 12).

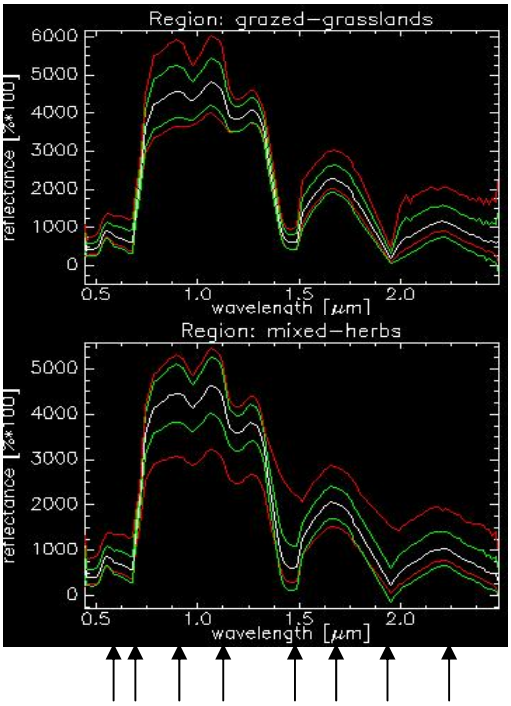

Figure 12. .. Bands selected to make the LSU classification, correspond to the wavelengths 550, 650, 900, 1100, 1470, 1650, 1900 and 2230 nm.

Table 10. Wavelength, spectral region, dominating factor controlling reflectance and absorption properties of the bands used in the Linear Spectral Unmixing Classification

Hymap Band (/126)	**Wavelength (nm)**	**Spectral region**	**Dominating factor controlling leaf reflectance**	**Primary absorption bands**
10	550	Green (VIS)	Leaf pigments	
15	650	Red (VIS)	Leaf pigments	Chlorophyll absorption
32	900	Near InfraRed	Cell structure	
45	1100	Near InfraRed	Cell structure	
68	1470	Shortwave InfraRed 1	Water content	Water absorption
82	1650	Shortwave InfraRed 1	Water content	
95	1900	Shortwave InfraRed 2	Water content	Water absorption
110	2230	Shortwave InfraRed 2	Water content	

In the case of Mixture Tuned Match Filtering the band selection is done automatically getting the Minimum Noise Fraction eigenvalues. The graph in Figure 13 shows the relevance of the 126 eigenvectors created from the Minimum Noise Fraction process. According to ENVI online help, eigenvalues greater than 1 contain data meanwhile eigenvalues smaller than 1 contain noise (ENVI, 2003). In this study, only eigenvalues greater than 5 were used, as the curve was reaching the asymptote at that point. Then, the first 8 bands were chosen to make the MTMF classification.

The end-member collection to make the classification was done from the field samples pixels in the case of grasslands and mixed herbs; and manually in the map for the rest of the end-members (soil, shrubs, forest and agricultural crops). This manual collection was helped by knowledge about the area and aerial pictures.

Because of the heterogeneity of the area and the overlap of spectral signatures of different PFTs (Figure 14), the classification did not performed in a totally constraint way. Masks were applied to avoid values of the output classes below 0 and over 1 per pixel.

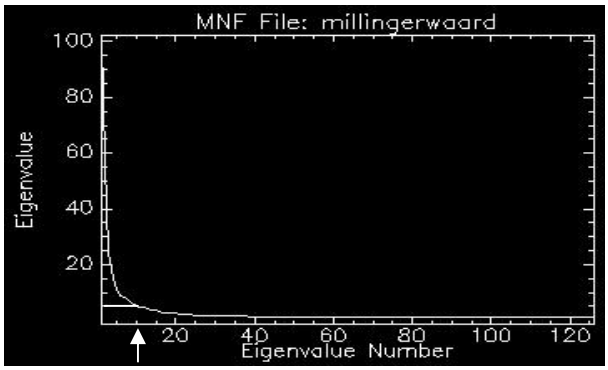

Figure 13. .. Eigenvalues correspondent to the Minimum Noise Fraction analysis.

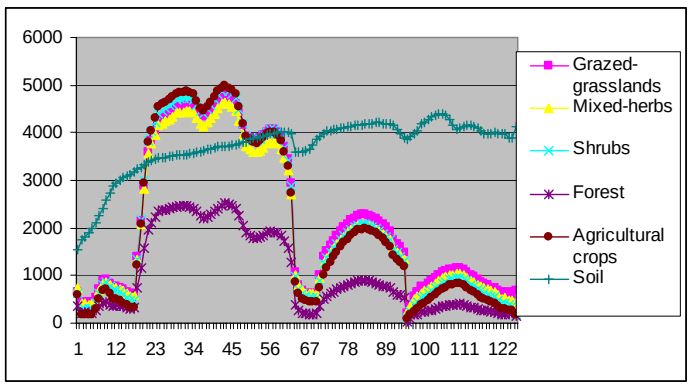

Figure 14. .. Mean spectra of the six end-members used in the plant functional type's classification.

A test of the error was carried out, checking if non-possible values (above 1 and below 0) were spread all over the image or were PFT-related. As the affected pixels were present all over the area and in a low percentage, the error was attributed to the difficulty of the classification.

To check the reliability of the two classification methods, the 21 plots from the field work were analyzed.

3.6 STATISTICAL APPROACHES ESTIMATING BIOMASS

The first part of the methodology applied in this case study evaluates the performance of the statistical approaches estimating biomass in the study area. Four vegetation indices were selected to be later related with measured vegetation biomass in Millingerwaard. The four indices derived from the 2004 Hymap image were the Normalized Difference Vegetation Index (NDVI), the Soil Adjusted Vegetation Index (SAVI), the Weighted Difference Vegetation Index (WDVI) and the Simple Ratio (RSR). The selection of these four vegetation indices was done based on literature review about similar researches and studies carried out previously in the area. The NDVI has been related with biomass by several authors before (Foody *et al.*, 2003; Zheng *et al.*, 2004; Rahman *et al.*, 2005). The SAVI and the WDVI correct for the soil background, what can be important in this area because although being of a high fractional vegetation coverage bears mostly short species. The gaps between the vegetation could influence the signal with the soil reflectance. The LAI was calculated in the forested part of the area derived from RSR index (Chen *et al.*, 2002) getting high accurate results (Mengesha, 2005), so RSR was used to check its possible relationship with the biomass in the low-vegetation part.

The four vegetation indices were obtained for each sample location and compared to the dry biomass weight from the aboveground vegetation collected in the same location in the field.

The coordinates from the field samples where first converted from the Dutch Rijks Driehoek (RD) coordinate system into WGS-84 projection system. The field samples were then overlaid on the Hymap image to get the values of the vegetation indices corresponding to each sampling coordinate. Some uncertainties were found as the

location of each sample point was not the central point of a pixel. The maximum deviation between the sampling coordinates and the respective pixel centre is 2.91 meters. Complete information about the pixel and sampling centres differences can be found in Appendix 2 (Table 21).

In the regression analysis, evidence about the dependence of the biomass with the plant functional type and the managing methods (e.g. grazing) was found. This evidence was checked to be present also in the results of the image of the following year (2005) to demonstrate its consistency. In previous studies this differentiation between grasslands species and other herbaceous species has been done (Nichol and Lee, 2005).

The process to get the relationship between the four vegetation indices and biomass was done using a cross-validation technique in which an equation is got from the VI-biomass relationship of 20 samples while validating with the 21st. This process is done per PFT with all the samples. The Root Mean Square Error of the Cross Validation (RMSECV) and the Root Mean Square Error of Prediction (RMSEP) were calculated.

$$RMSEP = \sqrt{\left(\frac{\sum (r - r')^2}{n}\right)}$$

Where:

r= Measured biomass in the field.

r'= Corresponding biomass according to the regression line.

n= Number of biomass samples included in the analysis.

The RMSECV analyses the difference in between the value of a sample and the predicted value at that point depending on the rest of the samples. Then, the validation is independent in this case from the field sampling in each point.

$$RMSECV = \sqrt{\left(\frac{\sum (r - r')^2}{n - 1} \right)}$$

Where:

r= Measured biomass in the field.

r'= Corresponding biomass according to the regression line calculated from the rest of the measurements from the field.

n= Number of biomass samples included in the analysis.

The bands used to calculate the different vegetation indices were chosen because their reliability in the quality assessment of the image carried on in previous studies (Liras-Laita, 2005; Mengesha, 2005). Table 11 gives an overview of the used bands.

Table 11. Hymap bands and wavelength used in the calculation of the vegetation indices

	Wavelength (nm)	**Hymap band (total 126)**
Green (G)	497	5
Blue (B)	573	10
Red (R)	650	15
Near Infra-Red (NIR)	846	28
Short-Wave Infra-Red (SWIR)	1661	82

3.6.1 NDVI analysis

The formula used for calculating the Normalized Difference Vegetation Index (NDVI) was:

$$NDVI = \frac{NIR - Red}{NIR + Red}$$ (Rouse, 1974)

3.6.2 WDVI Analysis

The Weighted Difference Vegetation Index (WDVI):

$$WDVI = NIR - a \times Red.$$ (Clevers, 1989)

Where a is the ratio of NIR to Red in the soil, it was calculated from a bare soil pixel in the research area and its value corresponds to 1,928. The bare soil reflectance curve can be found in Figure 26 (Appendix 3). It is hard to find a bare soil pixel inside the study area because of the high vegetation coverage; the spectrum corresponds to a pixel from a crossing path.

3.6.3 SAVI Analysis

The Soil Adjustment Vegetation Index (SAVI) was calculated according to:

$$SAVI = \frac{NIR - Red}{NIR + Red + L}(1 + L)$$

Where L is the soil adjustment factor

(Huete, 1988)

From literature is known that the most common value used for L that has been used is 0, 5 so that was the value considered in this study as well.

3.6.4 RSR Analysis

The Reduced Simple Ratio (RSR) was taken from Chen *et al*. in 2002

$$RSR = \frac{\rho NIR}{\rho RED}\left(1 - \frac{\rho SWIR - \rho SWIR\min}{\rho SWIR\max - \rho SWIR\min}\right)$$

(Chen *et al.*, 2002)

The SWIR (Short Wave Infra-Red band) is considered to be band 82 corresponding to 1661 nm; the SWIR (band 82) minimum and maximum reflectance values in the vegetated area respectively are 0 and 0.4051.

The regression analysis was done for three sample sets (See Figure 26 in Appendix 3):

- Whole dataset (n=21).
- Grazed-grassland (n=7).
- Herbaceous vegetation (n=14)

Linear ($y= ax + b$) and exponential ($y= a \,.\, e^{bx}$) or logarithmic ($y= a.Ln(x) + b$) relationships were considered as in previous studies it is demonstrated these are the ones explaining the relationship between vegetation indices and quantitative variables (Clevers, 1989).

For every relationship R^2, RMSEP and RMSECV were calculated to evaluate the strength of the relationship.

3.6.5 Biomass map

The biomass map was constructed with the results of the regression analysis applying the best relationship proportionally per coverage of PFT per pixel. The general formula applied was:

$$B = \left[Best.relation(GR) \times (\%grasslands)\right] + \left[Best.relation(MH) \times (\%mixed - herbs)\right]$$

In the formula the best relationships VI-Biomass from previous step are used. The biomass estimated value was compared with the measured biomass from the field.

3.7 RADIATIVE TRANSFER MODELS

The coupled model PROSPECT-SAIL (Jacquemoud, 1993) (Section 2.3.3) was used as a second approach to estimate biomass in the research area. The version of the model used is implemented in Interactive Data Language (IDL) with a user interface. In Table 12 and Table 13 an overview of the input parameters of the two models is presented.

General average values from the main species per PFT were taken from literature review (Haselwimmer, 2005; Liras-Laita, 2005). The input parameters are highly species specific and the information available about the values is limited. Therefore, assumptions had to be made while applying these models in heterogeneous areas as there is no information available about the input parameters of all the species present.

Table 12. Overview of the input parameters for Prospect model, their units and description.

Prospect model		
Parameters	**Units**	**Description**
Structural parameter (N)	dimensionless	Number of compact layers specifying the average number of air / cell walls interfaces within the mesophyll
Chlorophyll a and b content (Cab)	mg/cm2	Concentration of Chlorophyll a and b in the leaves
Leaf water content (Cw)	cm	Water content in the leafs in units of thickness of layer of water per surface area
Leaf dry mass content (Cm)	g/cm2	Dry matter (protein+ cellulose+hemicellulose + sugar + starch + lignin) per unit area
Leaf brown pigment content (Cb)	relat.units	Brown pigment concentration

Table 13. Overview of the input parameters for Sail model, their units and description.

Sail model		
Parameters	**Units**	**Description**
Leaf Area Index (LAI)	dimensionless	Total one-sided leaf area per unit layer area
ALA	degrees	Average leaf angle
HS	dimensionless	Hot Spot parameter
VZ	radians	View Zenith angle
SZ	radians	Sun zenith angle
Az	radians	Azimuth angle
Soil spectrum	%reflectance	Background soil spectrum
Leaf spectrum	%reflectance	Spectrum of a leaf corresponding to the simulated canopy

The first assumption made deals with the number of species considered in the model inversion. In this case study, four species where taken into account: *Calamagrostis epigejos*, *Urtica dioica*, *Rubus caesius* and *Trifolium repens*. The election of the species is based on the input data values available from literature. The rest of the species present are assumed to be represented by one of the four species used in the analysis. In the case of the Grazed-grasslands, they are all represented by *Trifolium repens*; *Calamagrostis epigejos* and *Urtica dioica* represent the herbaceous species and *Rubus caesius* is the shrub species used.

The second assumption made is that each single pixel is considered homogeneous. Then, the output from the model inversion will be a combination of input parameters correspondent to one species.

The two input parameters *Dry matter content* from the leaf level-Prospect model and the *LAI* from the canopy level-Sail model are directly related to biomass content in the canopy.

A sensitivity analysis of the model was performed for these two input parameters (LAI and Dry matter content) towards checking if the models answered to variations in those inputs. Moreover, the relationship between this inputs and the vegetation indices coming from the simulated spectra were also studied.

3.7.1 SENSITIVITY ANALYSIS

The sensitivity analysis was carried out with the following steps:

- Investigation of the common values of the studied variable.
- The other input variables in the models are set in fixed values per species.
- The value of the studied variable is changed each time the model is run.
- With the resulting spectra, variations depending on the studied variable are checked and VI are calculated and also compared with the variable changed.
- When the sensitivity analysis shows a variation of the output with a change in a variable, it means the model is sensitive to the magnitude of such change n the variable independently from the others.

LEAF AREA INDEX

The sensitivity analysis was done for four species, namely *Calamagrostis epigejos*, *Urtica dioica*, *Rubus caesius* and *Trifolium repens*. The first three species were classified as belonging to mixed-herbs PFT while the fourth is grassland species.

The Prospect model was first run for them, having as output the estimated reflection of the leaves in each case out of average input values. Then, SAIL model was carried out six times per specie with different values of LAI: 0.3, 1, 2, 3, 4 and 5. An overview of the input values used in the LAI sensitivity analysis is given in Table 14.

Table 14. Parameters used for the LAI sensitivity analysis

		Calamagrostis epigejos	**Urtica dioica**	**Rubus caesius**	**Trifolium repens**
Prospect	**N**	1.4	1.5	1.5	1.875
	Cab (mg/cm2)	30	70	75	46.7
	Cw (cm)	0.008	0.008	0.01	0.01
	Cm (g/cm2)	0.003	0.002	0.005	0.003014
	Cb	0.05	0.1	0.1	0.05
Sail	**LAI**	0.3, 1, 2, 3, 4, 5	0.3, 1, 2, 3, 4, 5	0.3, 1, 2, 3, 4, 5	0.3, 1, 2, 3, 4, 5
	ALA (deg)	30	30	30	30
	HS	0.0125	0.0125	0.00319	0.0125
	VZ (rad)	0	0	0	0
	SZ (rad)	0.574	0.574	0.574	0.574
	Az (rad)	0	0	0	0
	DF	0	0	0	0

DRY MATTER CONTENT

Another sensitivity analysis was carried out to see how changes in the dry matter content in the leaves affect the canopy reflectance. In this case it is an input of the Prospect model the one that is studied but at the canopy level (Sail model). Five different values of Dry matter content (Prospect input) were used and the values of Sail model were fixed in average ones.

The average values for all the inputs and the values used for C_m (Dry matter content in the leaves) are resumed in Table 15.

With the results of the sensitivity analysis, a correlation study between the variables *LAI* and *Dry matter content* with the VI was done. The vegetation indices were calculated from the spectra got from the model for each simulation input parameters.

Table 15. Input parameters for Dry matter content sensitivity analysis

		Calamagrostis epigejos	**Urtica dioica**	**Rubus caesius**	**Trifolium repens**
Prospect	**N**	1.4	1.5	1.5	1.875
	Cab (mg/cm^2)	30	70	75	46.7
	Cw (cm)	0.008	0.008	0.01	0.01
	Cm (g/cm^2)	0.001, 0.002, 0.003, 0.004, 0.005	0.001, 0.002, 0.003, 0.004, 0.005	0.001, 0.002, 0.003, 0.004, 0.005	0.001, 0.002, 0.003, 0.004, 0.005
	Cb	0.05	0.1	0.1	0.05
Sail	**LAI**	3	3	3	3
	ALA (deg)	30	30	30	30
	HS	0.0125	0.0125	0.00319	0.0125
	VZ (rad)	0	0	0	0
	SZ (rad)	0.574	0.574	0.574	0.574
	Az (rad)	0	0	0	0
	DF	0	0	0	0

3.7.2 MODEL INVERSION USING LOOK UP TABLES

The way of getting biophysical variables from radiative transfer models is using modelling inversion (Atzberger, 2004). In this case the variables to get from the inversion are C_m and *LAI*. The inversion method that is applied in this case study is based on look-up-tables (Section 2.4 "model inversion" of this report gives an introduction) because of its simplicity at the same time it performs well (Weiss *et al.*, 2000). In this case, the inversion procedure was done only for the field work sample points. The aim of doing this inversion was to know if the technique could be used to estimate biophysical variables in a heterogeneous area as Millingerwaard. Four look up tables were prepared, each of them corresponding to one of the main four species in the area: *Trifolium repens*, *Urtica dioica*, *Calamagrostis epigejos* and *Rubus caesius*.

The procedure followed to generate the look-up-tables was (Figure 15):

- Set fixed values for all the input parameters but C_m and *LAI* per species.

- Find out the most common values of C_m and *LAI* respectively per species. The number of simulations will depend on the number of values considered per C_m and *LAI*. The possibilities of simulating the image spectra increase with the number of simulations done.

- Run the PROSPECT/SAIL model with each possible combination of C_m and *LAI* coming from the previous step.

- Extract from each simulated spectrum the eight bands chosen for the inversion corresponding to the wavelengths: 550, 650. 900, 1100, 1470, 1650, 1900 and 2230 nm. These bands have been chosen as representative of the crop spectra in the study area with the same criterion as the selection for the LSU classification procedure. The results of the inversion will directly depend on these bands.

- Build a table in which each row gathers the eight bands reflectance values coming from the simulated spectrum of each combination of C_m and *LAI*.

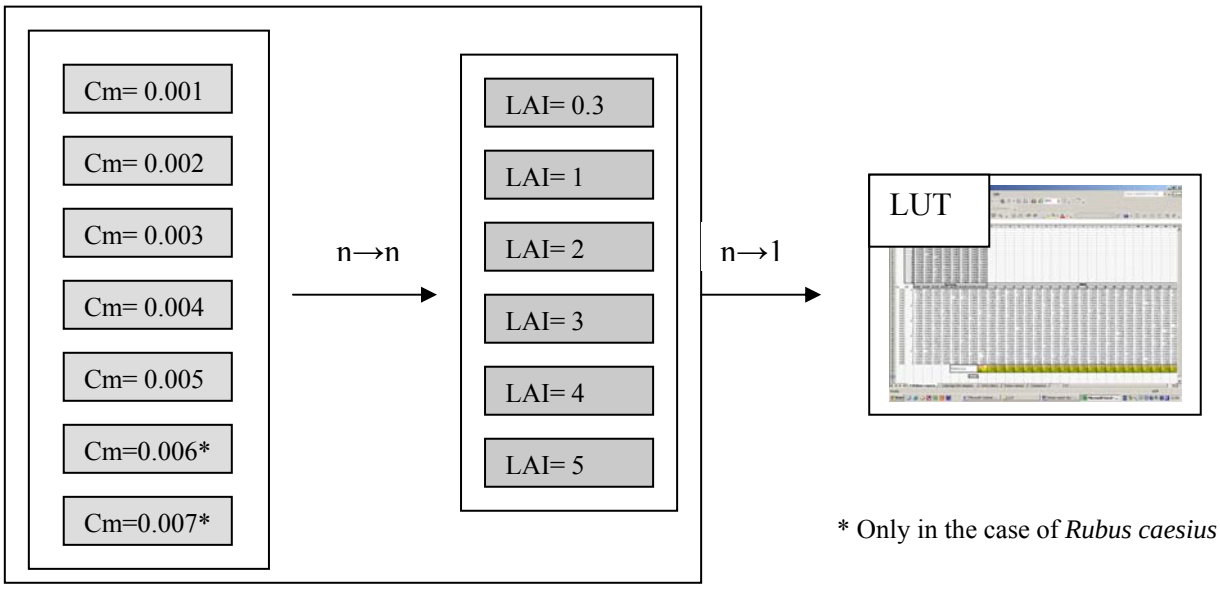

Figure 15. .. Look-up-table generation scheme. n→n means all the members of the first rectangle were related independently with all the members of the second. n→1 means all the combinations were plot in a single LUT.

The look-up-tables gather the spectra coming from simulations with Prospect-Sail model for different values of Leaf Area Index and Dry matter content. A total of 30 simulations were done for *Trifolium repens*, *Urtica dioica* and *Calamagrostis epigejos* respectively and 42 for *Rubus caesius*.

Every sample plot spectrum was compared with each of the 132 simulation spectra and the Root mean square error of prediction (RMSEP) calculated for each comparison. The minimum RMSEP correspond to the minimum distance between the measured and the simulated spectra. Then, the C_m and *LAI* values used for such simulation are supposed to be the correspondents with the measured spectra.

After getting the simulated values of C_m and *LAI* per plot, the estimated leaf dry biomass of the plots is calculated by multiplying $LAI * C_m$. This estimated biomass is then compared with the measured biomass from the field. Estimated biomass is the dry biomass from the leaves. The measured biomass is both leaves and woody part dry biomass. Then, they cannot be directly compared. Nevertheless, they should be correlated as the measured biomass in the field is the biomass of the leaves plus the biomass of the stems and woody part.

4 RESULTS

4.1 PFT Classification

The resulting maps after applying the MTMF and LSU classification techniques for the PFT are presented in Figure 16. The classification maps show that using the whole spectrum does not mean the classification performs better. In the classification done using 8 bands (maps 1 and 3), there is more patchiness of classes than in the classification done with all the bands in the spectra. This difference can be due to the use of noisy bands of the spectrum. According to the classification technique, LSU overestimate forest (in blue) that is confined to the eastern part in the reality. Mixed-herbs are underestimated on the other hand.

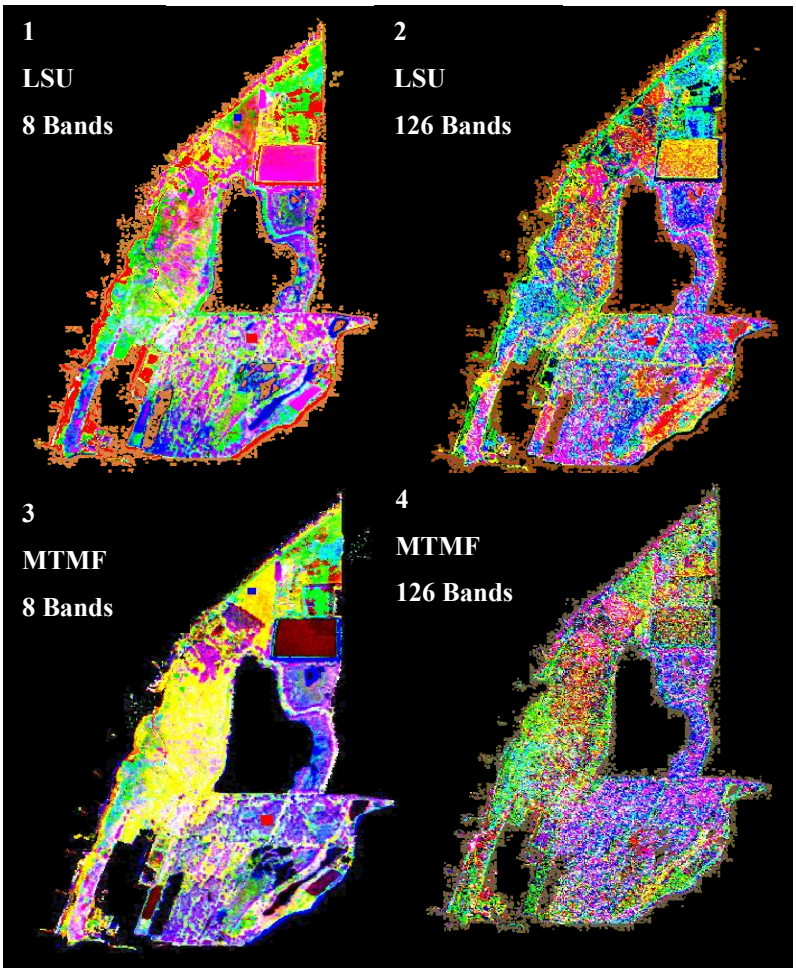

Figure 16. .. Linear Spectral Unmixing (1 and 2) and Mixture Tuned Match Filtering (3 and 4) comparison. In the figure, grasslands are represented in green, mixed-herbs in red and forest in blue. 1 and 3 were classified with 8 bands and 2 and 4 with whole spectrum. Validation of the classification of the sample plots with MTMF and LSU respectively

Table 16. Estimated fractional coverage of Grasslands and Mixed-herbs from MTMF classification and LSU classification in the sample points.

MTMF			**LSU**		
GRASSLANDS			**GRASSLANDS**		
Location	**Class-grasslands**	**Class-mixed-herbs**	**Location**	**Class-grasslands**	**Class-mixed-herbs**
2	0.9185	1	2	0.5514	0
5	0.6481	0.6318	5	0.7062	0
13	1	0	13	1	0.8567
14	0.9293	0	14	1	0
15	0.5202	0.5875	15	0.3114	0
19	0	1	19	0.9331	0
21	0.8172	0.8425	21	0.6263	0
MIXED-HERBS			**MIXED-HERBS**		
Location	**Class-grasslands**	**Class-mixed-herbs**	**Location**	**Class-grasslands**	**Class-mixed-herbs**
3	0.8926	1	3	0.5185	0.1958
4	0.7601	1	4	0.3601	0.0468
6	0.5136	0.7022	6	0.3182	0.2227
7	0.4433	1	7	**0**	**0.3911**
8	0.7129	1	8	**0.0251**	**0**
9	0.9156	1	9	**0.1069**	**0**
10	0.8143	1	10	**0.0457**	**0**
11	0.7727	1	11	**0**	**0**
12	0.1863	0.9786	12	**0**	**0.0199**
16	0	1	16	0	1
17	0.4435	0.525	17	**0.2065**	**0**
18	1	0	18	1	0.7414
20	0.3921	0.2884	20	0.381	0
22	0.6389	0.4712	22	0.6657	0

Table 16 compares the results of the classification with the real classes in each sample point. The values 1 and 0 correspond to the set values after masking above 1 and negative values respectively. The values in bold correspond to points not classified as

grasslands or mixed-herbs with LSU method. Plots 8, 12 and 17 were classified as forest, plots 9, 10 and 11 as shrubs and plot 7 as agricultural area. With MTMF method, all the sample points were classified as grasslands or mixed-herbs.

The validation shows how the endmembers were not spectrally independent enough to be properly classified. Frequency distribution plots were prepared for both grazed-grasslands and mixed-herbs (Figure 17). They represent how mixed-herbs have been classified as more abundant in general. The picks in values 0 and 1 show the amount of pixels that had to be masked out because of having negative or above 1 values after the classification.

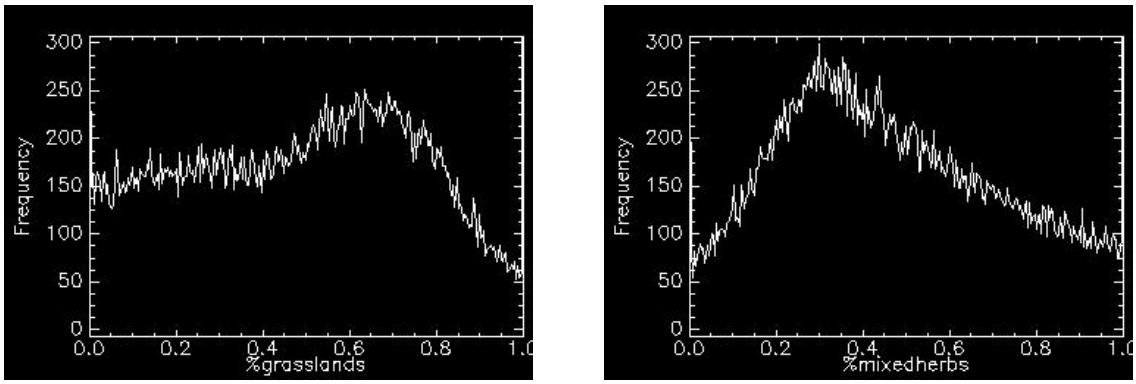

Figure 17. .. Frequency distribution of Grazed-Grasslands and Mixed herbs from MTMF classification.

4.2 STATISTICAL ANALYSIS

4.2.1 VEGETATION INDICES MAPS

The maps coming from the calculations of the four vegetation indices are shown in Figure 18 and the minimum and maximum values of each vegetation index in the Millingerwaard are summarized in table 17.

Table 17. Maximum and minimum value of each vegetation index.

Index	Minimum	Maximum	Mean	Stdev
NDVI	0	0.8913	0.0498	0.1837
WDVI	-4.147	5.5687	0.6289	1.3438
SAVI	-0.0163	0.1572	0.0059	0.0221
RSR	0	11.826	0.3534	1.3592

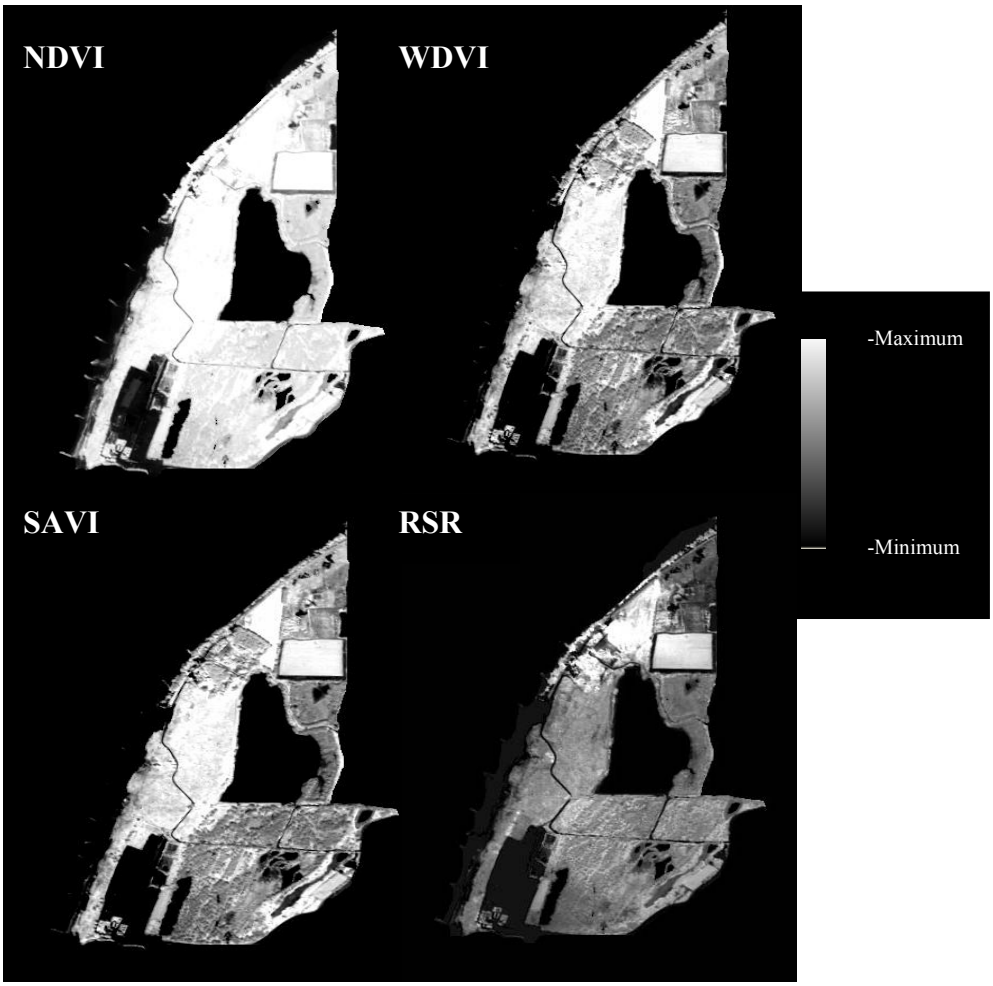

Figure 18... Vegetation index' maps calculated for the study area.

In general, in the vegetation index maps (Figure 18), we can see how the agricultural areas as the ones in the north with the shape of a rectangle and a triangle show the highest value (lightest). The forest, on the other hand, has the lowest values as can be seen in the eastern part of the area. The western area is where more grasslands and mixed-herbs are present; they have high NDVI, WDVI and SAVI. In the case of the RSR, nevertheless, the values are similar to the ones of the forest.

4.2.2 STATISTICAL PART: Correlation VI-Biomass

After correlating the values of the vegetation indices of the sample pixels with the measured biomass values of the sampling locations, VI-Biomass relationships were derived. The results of the correlation analysis with linear regression are presented in Table 18. The values for exponential and logarithmic regression can be found in Table 19.

Table 18. Vegetation indices-biomass correlation analysis overview. Linear regression (y=ax+b). r^2=correlation coefficient, SEP=Square Error of Prediction, SECV=Square Error of the Cross-Validation.

			LINEAR REGRESSION				
VI	**PFT**	**n**	**a**	**B**	**r^2**	**SEP**	**SECV**
NDVI	Grazed-Grasslands	7	-0.0001	0.7796	0.0577	164.26	280.55
	Mixed-herbs	14	0.0003	0.5338	0.4321	160.39	178.75
	All	21	0.0002	0.6638	0.1381	231.84	251.53
WDVI	Grazed-Grasslands	7	-0.0026	39,414	0.2452	147.01	201.31
	Mixed-herbs	14	0.0035	10,125	0.559	141.34	163.41
	All	21	0.0014	24,814	0.127	233.33	262
SAVI	Grazed-Grasslands	7	0.00007	0.1231	0.3702	134.28	189.4
	Mixed-herbs	14	0.00008	0.0558	0.5713	139.36	163.32
	All	21	0.00005	0.0889	0.1091	235.71	266.51
RSR	Grazed-Grasslands	7	-0.0023	41,702	0.0706	163.13	281.23
	Mixed-herbs	14	0.0033	19,737	0.2338	186.31	211.88
	All	21	0.0019	28,722	0.0998	236.93	257.27

Table 19. Vegetation indices-biomass correlation analysis overview. Exponential and logarithmic regression. In red, the best correlations found for mixed-herbs and grasslands respectively are shown. These correlations will be later used to calculate the biomass map.

				EXP-LOG REGRESSION				
VI	**PFT**	**n**	**TYPE**	**a**	**b**	**r^2**	**SEP**	**SECV**
NDVI	Grazed-Grasslands	7	EXP	0.7704	-0.0002	0.0438	171.82	341.78
	Mixed-herbs	14	LOG	0.2367	-0.729	0.62	163.08	179.62
	All	21	LOG	0.058	0.392	0.1063	242.21	264.98
WDVI	Grazed-Grasslands	7	EXP	39,019	-0.0008	0.249	153.11	215.37
	Mixed-herbs	14	LOG	**22,679**	**-11,236**	**0.7046**	150.02	173.77
	All	21	LOG	0.398	0.7674	0.0608	245.55	283.13
SAVI	Grazed-Grasslands	7	EXP	**0.1237**	**-0.0007**	**0.4057**	135.4	177.03
	Mixed-herbs	14	LOG	0.0477	-0.2008	0.6879	149.5	175.88
	All	21	LOG	0.0068	0.0618	0.0386	248.36	287.21
RSR	Grazed-Grasslands	7	LOG	0.4854	61,628	0.038	170.97	368.96
	Mixed-herbs	14	LOG	24,504	-11,589	0.3965	198.32	223.74
	All	21	LOG	0.7565	-0.07741	0.0939	248.08	271.13

The best correlation found for grazed-grasslands was the exponential with SAVI. The biomass of the mixed-herbs, nevertheless, was better correlated by a logarithmic relationship with WDVI (Table 19). That means the soil background is important in the total reflectance of the area, as these two indices are the ones that have it into account.

4.2.3 BIOMASS MAP

The biomass map was calculated (Figure 19) using for the Grazed-grasslands the relationship SAVI-Biomass and for the Mixed-herbs the relationship WDVI-Biomass. The formula applied per pixel to get the final map of biomass was:

$$B = \left[-616.18 \times Ln(SAVI - 1086.2) \times (\%grasslands)\right] + \left[215.51 \times e^{(0.3107 \times WDVI)} \times (\%mixed - herbs)\right]$$

This map shows the biomass corresponding to the grassland and herbaceous vegetation in the area. The lightest parts are where the biomass of grasslands and mixed-herbs plant functional types is higher and the darkest parts show were the biomass of the formers is low. Indeed, the darkest areas in the map correspond to the forested area, because the analysed plant functional types are less abundant.

In the corresponding frequency distribution (Figure 19), we can see the highest occurrence correspond to a biomass around 300 gr/cm^2.

A table with the comparison between estimated and field biomass values can be found in the appendix 3 (Table 22).

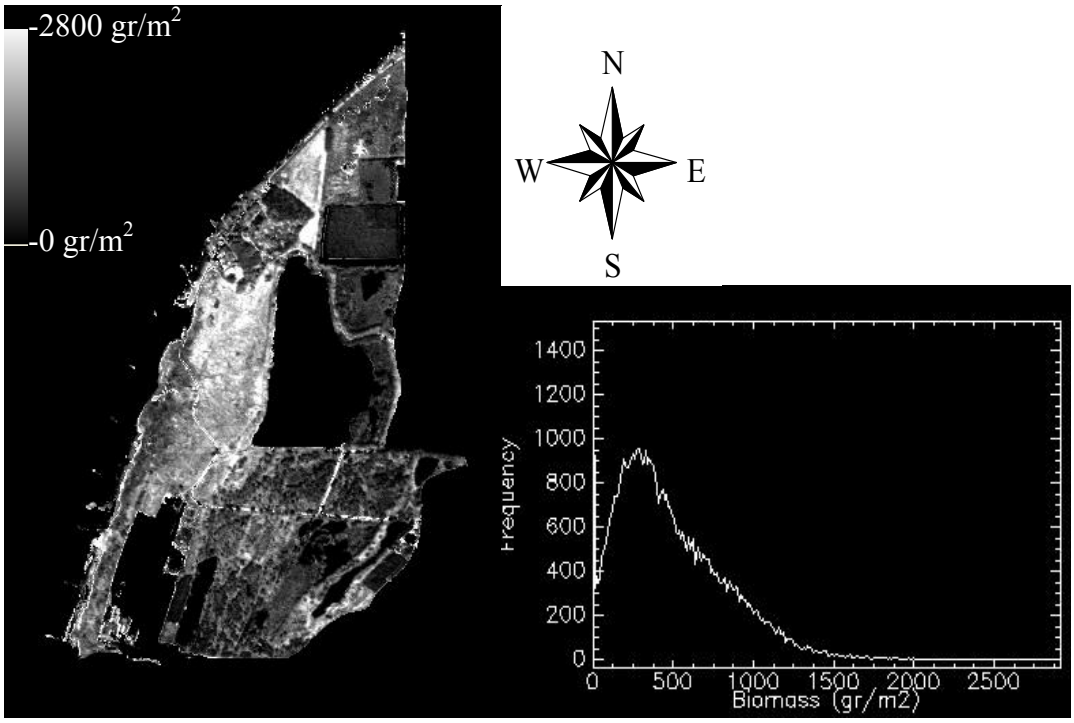

Figure 19. .. Biomass map obtained for Grazed-grasslands and Mixed-herbs' PFT. On the right, the corresponding frequency distribution.

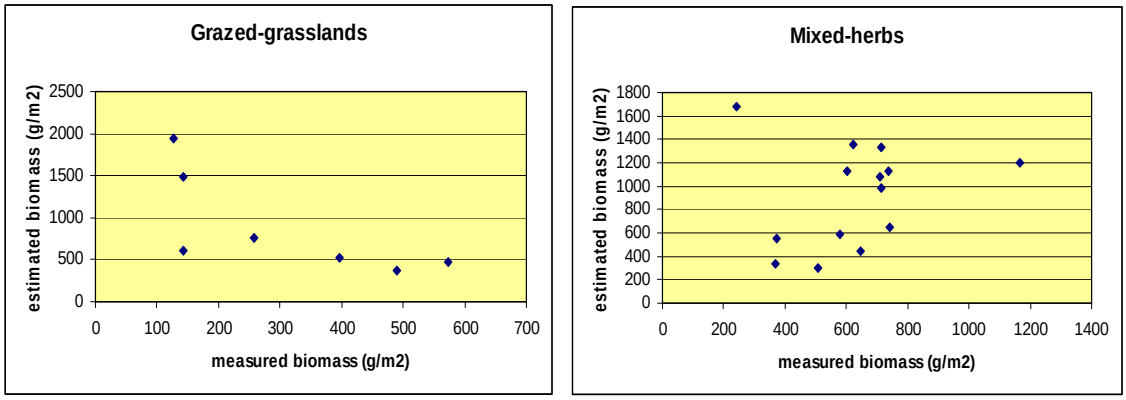

Figure 20. .. Comparison between estimated biomass with statistical methods and measured biomass in the field.

Figure 20 shows the comparison of the estimated biomass values with the measured values from the field. Estimated values have no correlation with the measured ones.

The correlation between estimated biomass with statistical approaches and measured biomass in the field can be improved increasing the number of sampling plots. If the number of sampling plots is higher, the vegetation is better represented so the correlation relationships are probably more stable.

4.3 RADIATIVE TRANSFER MODELS ANALYSIS

4.3.1 SENSITIVITY ANALYSIS

The PROSPECT/SAIL models were used to carry out a sensitivity analysis for four species. Figure 21 shows the variation in the spectra of the canopy depending on the LAI value. Figure 22 shows the same approach with the Dry matter content in the leaves.

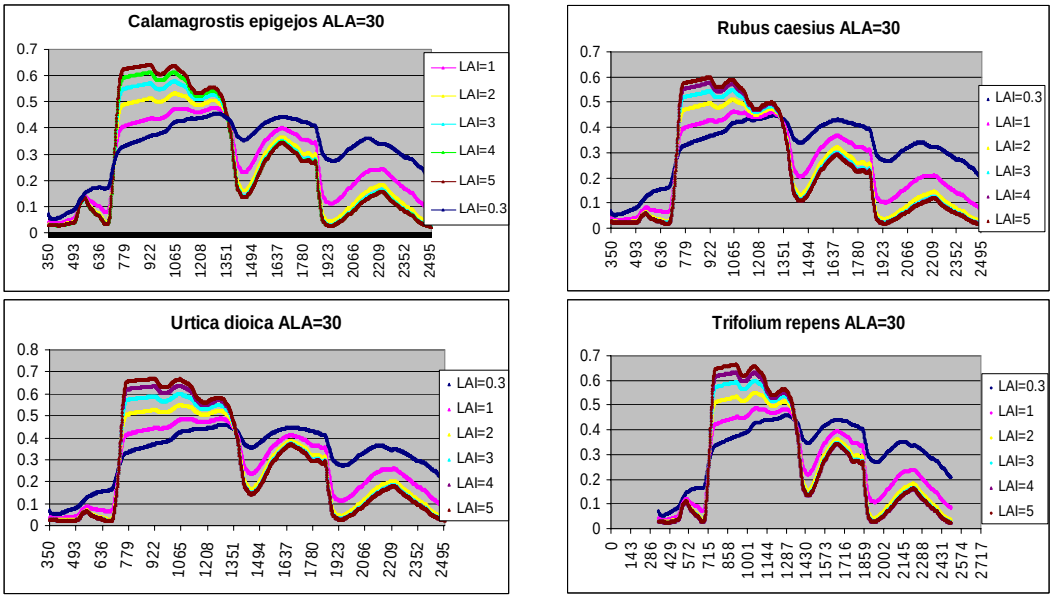

Figure 21. .. LAI Sensitivity analysis for *Urtica dioica, Trifolium repens, Calamagrostis epigejos* and *Rubus caesius*.

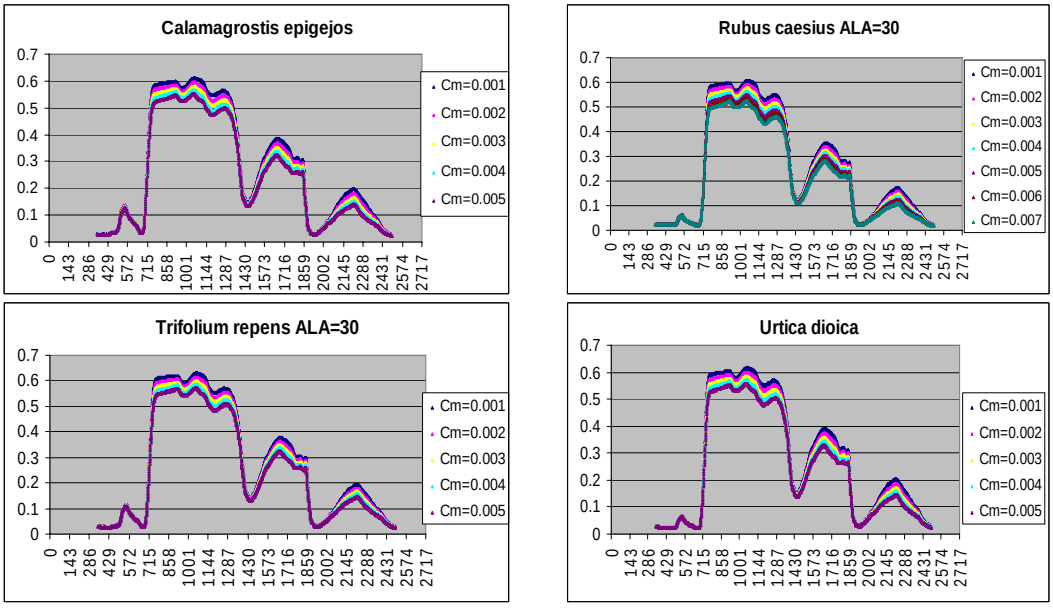

Figure 22. .. Dry matter sensitivity analysis results

From Figure 21, we can say the spectra of the canopy vary depending on the variation of LAI, what means the model is sensitive to this parameter. On the other hand, in Figure 22, the variation in between spectra of different Dry matter content is hardly visible.

From the simulated spectra, values for the vegetation indices were calculated and compared to LAI and Dry matter content (Figure 29, Appendix 4).

The vegetation indices grow exponentially with the increase of the LAI until reaching saturation. NDVI shows the lowest saturation level at a LAI=2 approximately. RSR is the vegetation index that shows more sensitivity to the variation of LAI. On the other hand, the vegetation indices decrease in a linear trend with the increase of the dry matter content in the leaves. In this case, we can see how the species *Urtica dioica* and *Rubus caesius* spectra are generally overlapping each other, probably due to their structural similarities. WDVI in this case show less sensitivity to the change in dry matter in the leaves than the rest of the vegetation indices studied. WDVI is more sensitive to the change in the NIR part of the spectrum than the rest of the indices. The NIR part of the spectrum reflects the multiple-scattering effects due to the structure of the vegetation. Thus, WDVI is more sensitive to variables in the canopy level than variables in the leaf level where no multiple-scattering is occurring.

4.3.2 RTM inversion

After creating the look-up-tables, each RMSEP was calculated per plot with all the different simulation spectra from the model. A table with the minimum RMSEPs per plot per LUT can be found in the appendix 4 (Tables 23 and 24).

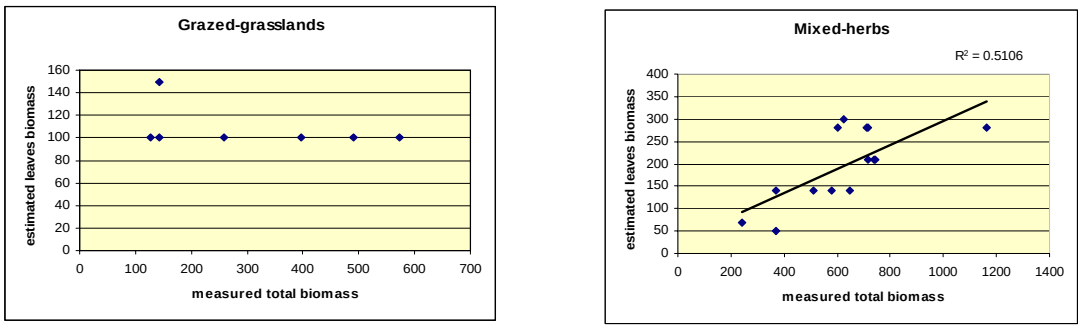

Figure 23. .. Correlation between estimated leaf biomass values and radiative transfer models and total measured biomass values in the field.

The grazed-grasslands field sample plots achieved the lowest value of RMSE with *Rubus caesius* simulations (Table 23). Nevertheless, in Figure 23, the graph corresponding to grazed-grasslands compares the measured biomass in the field and the estimated biomass assuming *Trifolium repens* is the only species present.

The inversion of the herbaceous plots resulted in all the plots estimated as *Rubus caesius* but one (plot number 16). Plots number 16 and 18 correspond to samples on the beach area with total vegetation coverage of 15% and 30% respectively. The estimated LAIs correspond to 1 what means the inversion performs in a realistic way.

The comparison of estimated biomass from the model inversion and measured biomass in the field was done by plotting the values in a graph per plant functional type. In figure 23, the two graphs for grasslands and mixed-herbs are shown.

For grasslands, no correlation was found. For mixed-herbs it looks the predicted values are correlated with the measured values (R^2= 0.5106).

Estimates of LAI in the study area were done in previous studies (Schmidt, 2005) derived from RSR (Chen *et al.*, 2002) with an empirical correlation RSR-LAI in the forest. In Figure 24, previous estimations of LAI in the area are compared with the estimations from this case study.

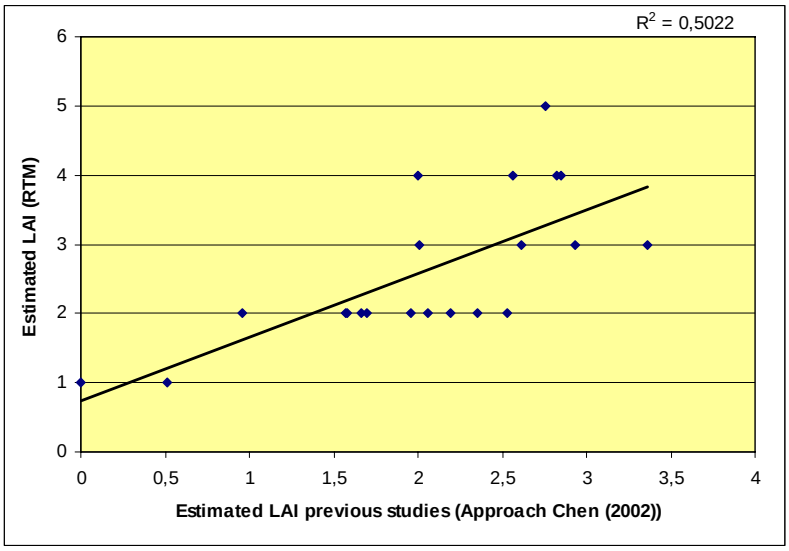

Figure 24... Comparison between LAI estimates of previous studies in the area with LAI estimates in this case study

5 DISCUSSION

5.1 STATISTICAL APPROACHES ESTIMATING BIOMASS

5.1.1 Vegetation index maps

The maps resulting from the vegetation indices calculation (Figure 18) give already an idea about the indices that best can estimate biomass in the research area. Having into account the high vegetation heterogeneity of the Millingerwaard, we can check if such heterogeneity can be detected in the maps. At a first glance, differentiation between different plant functional types (with the help of knowledge about the spatial distribution of such plant functional types in the area), can be detected in the four vegetation indices maps (Figure 18). Both the NDVI and the RSR maps look more homogeneous than the other two: WDVI and SAVI. This is a first overview of the performance of the different vegetation indices estimating biomass.

5.1.2 VI-Biomass relationship

Several authors suggest on theoretical and empirical grounds that the simple ratio is best related with LAI (Steinmetz, 1990) while others have supported the use of NDVI (Gallo *et al.*, 1993). In Figure 29 (Appendix 4), nevertheless we can see how NDVI is the index that reaches the saturation point at a lower LAI. The estimation of LAI is directly related with the estimation of biomass as both are quantitative biophysical variables.

In this case, the image used is a hyperspectral narrow-band image. From literature it is known that the narrow band combinations respond differently to a variation in biomass. (Mutanga, 2004). This can be due to the uncertainty in the determination of the Red band. In the case of the NIR band, as there is a plateau in typical vegetation spectra, there should be no problem.

Huete (1985) stated that the sensitivity of vegetation indices to the soil background is greatest with intermediate levels of vegetation cover (Huete *et al.*, 1985). At very high densities there is not enough soil signal emerging from the canopy to be of

significance (Huete, 1988). In the case of this study, although the coverage percentage is high, the dominant species in the area are short, so the soil reflectance has a higher influence than in the case of higher vegetation species as for example in forest areas. This could explain the good results with SAVI and WDVI in herbaceous vegetation.

In the cases of soil lines not substantially different from the normal assumed in the ratio indices SR (in which RSR is based) and NDVI, these indices give better results. On the contrary, in the cases in which the soil spectrum plays an important role, SAVI has given better results (Lawrence and Ripple, 1998). Analogously, WDVI is also supposed to be a good estimator like SAVI because it takes the soil background into consideration as well.

In the results of this research, the NDVI index was not good at predicting biomass in the area. Already in the map (Figure 18) is visible how there is no clear differentiation of features. The reason of this fact can be the lower saturation point of LAI for NDVI.

In dense vegetated areas where the coverage is high, the variation of biomass is only reflected in the NIR part of the spectrum. In high vegetation covered areas, the variation in biomass is only dependant on the quantitative variables as canopy height. These variables can only be detected by the scattering that at the same time is only detected by the NIR part of the spectra. Then, indices as the NDVI are not able to differentiate quantitative variables and tend to reach an asymptote in their relationship with such variables (in Figure 29 NDVI is the index with the lowest saturation LAI value around 2). The quantitative variables estimations in these areas would be helped with techniques as Lidar (Ni-Meister *et al.*, 2001).

Clevers already in 1989 and other authors later explained how the vegetation indices reached a saturation level in their relation with biophysical variables. This means they become insensitive to the increase of such variables at a certain point (Clevers, 1989; Thenkabail *et al.*, 2000). Given this limitation, there is a need to develop or improve techniques that can accurately estimate biomass in more densely vegetated areas. That is why radiative transfer models are being lately inverted to get biomass from other source different from vegetation indices.

The relationship in the case of WDVI and SAVI is far better than the one with NDVI (Table 19), that means that possibly the soil influence in the area is high. In the case

of the grasslands, where the relationship biomass-VI is quite weak, the soil influence can be important as the vegetation is short. Moreover, WDVI and SAVI are sensitive to the variation in the NIR part of the spectrum and the multiple-scattering phenomenon is only detected in this part of the spectrum. So in high vegetated areas, WDVI and SAVI are expected to estimate better quantitative variables.

The RSR index is considered to be directly related with the biophysical variable Leaf Area Index (LAI) (Chen *et al.*, 2002). In this case, the relationship of this index with biomass is not good (Tables 18 and 19).

The dependency of VI-biomass relation with the plant functional types can be justified by differences in plant and leaf structures. Herbs are non-woody vegetation so the dry weight is far smaller in comparison to shrubs. Furthermore, the vegetation indices give information about the vegetation health, so young healthy herbs would have high vegetation indices and very low biomass and woody not that healthy shrubs would have the contrary. Therefore, the relation between biomass and vegetation indices was derived per PFT.

The calculated biomass map using statistical approaches (Figure 19) looks like realistic. However, the biomass in the sample points is not well-estimated (Figure 20 and Table 22). This can be solved getting more accurate relationships what can be done by increasing the number of sample points in the field.

5.2 RADIATIVE TRANSFER MODELS

A simple approach was carried out to get biomass by inverting radiative transfer models. The main aim of this approach was to find out if it was suitable to retrieve quantitative biophysical variables in a heterogeneous area like Millingerwaard.

The sensitivity analysis showed the study species were similar in spectral characteristics and their reflectance curves overlapped (Figures 21 and 22). The models are more sensitive to LAI (input for the canopy level-model Sail) than to dry matter in the leaves (input for the leaf level-model Prospect).

The LUT were prepared only for four of the species present in the area. This decision was taken because of the lack of input information for other species. All the grasslands species were assumed to have identical spectrum as *Trifolium repens*. All the mixed-herbs were assumed to behave as one of those 3 species: *Urtica dioica*, *Calamagrostis epigejos* and *Rubus caesius*. In the inversion procedure, each pixel of the image was assumed to behave as if it was homogeneous in one of the four species considered.

As all the grassland plots were assumed to behave as if they were homogeneously covered by *Trifolium repens*, the estimated biomass from the inversion was not well correlated with the measured biomass in the field (Figure 26). This fact can also be seen in Table 23 (Appendix 4) where the grazed-grasslands plots do not achieve the lowest RMSEP with a simulated spectra coming from *Trifolium repens*. Indeed, *Trifolium repens* has an average fractional cover of 25.71% (Table 9) in the grazed-grasslands sample plots. Then, it can be concluded *Trifolium repens* is not representative enough of the grasslands PFT. The statistical results already showed it was difficult to well-estimate biomass for grasslands' PFT (Tables 18 and 19), and the PFT classification also achieved worse results for this PFT (Table 16).

The mixed-herbs biomass was better predicted (Figure 23). A first reason for this is that, this PFT was better represented as three species spectra were simulated. Secondly, *Rubus caesius* has a proportional fractional coverage of 34.93% and together with *Urtica dioica* and *Calamagrostis epigejos,* 57.5%. Moreover, more

simulations were included in the *Rubus caesius* LUT as the C_m values from literature had a bigger range (0.001-0.007 for *Rubus caesius* compared to 0.001-0.005 for the rest of the species).

5.3 PLANT FUNCTIONAL TYPES & HYDRAULIC RESISTANCE

5.3.1 PFT behaviour

It is source of further study the different sign in the VI-Biomass regression lines depending on the plant functional type. In the case of the Grazed-Grasslands the VI are inversely correlated with biomass (Figure 27). This inverse correlation was unexpected but at the same time consistent having into account the results of the sensitivity analysis of Dry Matter content with the PROSPECT-SAIL coupled model (Figure 22).

With the information of the resulting biomass map (Figure 19) and the Nikuradse value per PFT (Figure 3), an overall idea about the hydraulic resistance can be drawn. The lightest areas in the biomass map correspond to the highest biomass values. As the biomass map has been calculated only for grasslands and mixed-herbs, the highest values correspond to mixed-herbs (do not forget also the dominant species of shrubs *Rubus caesius* is included). According to Figure 3 (Section 2.2), the thorn-shrubs-subtype is the one with the highest hydraulic resistance. *Rubus caesius* is a thorn shrub, so the areas dominated by *Rubus caesius* then, have a high hydraulic resistance.

Looking at the map of Figure 19, we can say in the west-northern part of the image where the biomass is the highest (leaving apart the triangular agriculture field), the hydraulic resistance could also be relatively high. Meanwhile in the forested areas (dark areas) the hydraulic resistance is intermediate according to the values in Figure 3. The rest of the image in which biomass is low due to be dominated by grasslands, there must be almost not resistance to flooding.

5.4 Possibilities of up-scaling the methodology with Landsat images

The use of radiative transfer models for estimating biomass using Landsat images has not being assess by any author before. Nevertheless, its possibility is matter of future studies.

The methodology used in this thesis can be tried to be applied with Landsat images using unmixing classification techniques as suggested by Smith (1990) and sub-pixel model inversion as suggested by Weiss (2000).

In that way, the problem of the higher spatial resolution of Landsat images (30x30 m) compared with Hymap can be dealed by applying sub-pixel techniques.

6 CONCLUSIONS AND RECOMMENDATIONS

From this study we can conclude statistical approaches estimating biomass in a heterogeneous area are highly dependent on the presence of different plant functional types. The vegetation indices do not have comparable values between different vegetation types, and then there is no single absolute relationship applicable to the whole area.

The result applying statistical approaches estimating biomass looks realistic. Nevertheless, the estimated biomass values differ highly from the measured values in the field. The indices that had the best correlation with biomass were the Weight Difference Vegetation Index (WDVI) and the Soil Adjust Vegetation Index (SAVI).

Radiative transfer modelling inversion is a promising technique that needs large species-specific information. On the other hand is not site specific so there could be a possibility of up-scaling or applying this methodology to other similar vegetated areas.

Hydraulic resistance, as dependant on PFT can be spatially monitored. The spatial distribution of plant functional types can be an estimation of the spatial distribution of biomass. Moreover, in the cases in which a plant functional type's map is available, the biomass distribution can give information about the density of such PFT. Higher vegetation densities (understood as Biomass/volume) would mean higher hydraulic resistance.

Furthermore, when floodplains belong to nature areas and the ecological value is tried to be preserved, biomass mapping is a tool to quantify the environmental impact of the river management process (e.g. side channels).

The application of statistical approaches estimating biomass using Landsat images has been done in previous studies (Section 2.4). The recommendation in the case of heterogeneous natural areas is doing a previous PFT's classification.

Radiative transfer modelling has not been done with Landsat images yet. The main differences between Landsat and Hymap images are the spatial resolution (30x30 m in the case of Landsat and 5x5 m in the case f Hymap) and the availability of spectral

bands. To deal with the problem of spatial resolution, an unmixing classification and a subpixel-inversion technique can be applied.

Possible further applications with this research methodology

One possible application of the methodology applied in this case study is getting temporal biomass maps. In this way, monitoring land degradation in the area by means of loss of productivity can be assessed. Moreover, it can be studied such degradation depending on each plant functional type.

In a similar way, further study can be done concerning relative growth and the impact of different external factors in such growth. By these external factors is meant not only climate conditions but also physical conditions as soil type or contamination, slope, water availability etc.

The hydraulic resistance analysis can be an approach suitable for erosion-affected areas, for example Mediterranean countries; so it would be possible to fight against violent flooding and consequent loss of soil structure.

Some recommendations for similar future studies

In relation with the field sampling design, it should be done assuring enough representation of all the plant functional types present.

Before biomass cutting, spectral measurements of the sampled area should be made. In this way, the vegetation indices derived from these spectral signatures would be better correlated with the biomass samples. Then, heterogeneous sampling plots would not give problems of representation of the biomass samples.

Moreover, if samples are weighted in wet and dry conditions, further studies about influences of water content in vegetation indices could be done (Ceccato *et al.*, 2002). Weighting homogeneous species samples separating woody part from leaves, would provide leaves/total biomass relationship. If the former relationship is available, the biomass mapping by inversion of radiative transfer models could be done in terms of total biomass instead of leaves biomass.

A sub-pixel model inversion can be tried so the assumption of treating each pixel as species-homogeneous would not need to be taken (Weiss, 1990).

7 REFERENCES

Aase, J. K.; Siddoway, F. H. (1981). "Assessing winter wheat dry matter production via spectral reflectance measurements." Remote Sensing of Environment **11**(4): 267-277.

Atzberger, C. (2004). "Object-based retrieval of biophysical canopy variables using artificial neural networks and radiative transfer models." Remote Sensing of Environment **93**(1-2): 53-67.

Boardman, J. W. (1998). Leveraging the High Dimensionality of AVIRIS Data for improved Sub-Pixel Target. Unmixing and Rejection of False Positives: Mixture Tuned Matched Filtering. 5th JPL Geoscience Workshop, Pasadena, CA.

Braun-Blanquet, J. (1951). Pflanzensoziologie. Grundzuge der Vegetationskunde. Wien.

Calvao, T.; Palmeirim, J. M. (2004). "Mapping Mediterranean scrub with satellite imagery: Biomass estimation and spectral behaviour." International Journal of Remote Sensing **25**(16): 3113-3126.

Ceccato, P.; Gobron, N.; Flasse, S.; Pinty, B.; Tarantola, S. (2002). "Designing a spectral index to estimate vegetation water content from remote sensing data: Part 1: Theoretical approach." Remote Sensing of Environment **82**(2-3): 188-197.

Chen, J. M.; Pavlic, G.; Brown, L.; Cihlar, J.; Leblanc, S. G.; White, H. P.; Hall, R. J.; Peddle, D. R.; King, D. J.; Trofymow, J. A.; Swift, E.; Van der Sanden, J.; Pellikka, P. K. E. (2002) "Derivation and validation of Canada-wide coarse-resolution leaf area index maps using high-resolution satellite imagery and ground measurements." Remote Sensing of Environment **80**(1): 165-184.

Clevers, J. G. P. W. (1989). "The application of a weighted infrared-red vegetation index for estimating leaf area index by correcting for soil moisture." Remote Sensing of Environment **29**(1): 25-37.

Cohen, W. B.; Maiersperger, T. K.; Gower, S. T.; Turner, D. P. (2003). "An improved strategy for regression of biophysical variables and Landsat ETM+ data." Remote Sensing of Environment **84**(4): 561-571.

Cramer, W. (1999). "Comparing global models of terrestrial net primary productivity (NPP): introduction." Global Change Biology **5**(Suppl.1): iii-iv.

Cramer, W.; Bondeau, A.; Kicklighter, D. W.; Moore III, B.; Schloss, A. L.; Churkina, G.; Nemry, B.; Ruimy, A. (1999). "Comparing global models of terrestrial net primary productivity (NPP): Overview and key results." Global Change Biology **5**(SUPPL. 1): 1-15.

Daughtry, C. S. T.; Walthall, C. L.; Kim, M. S.; Brown de Colstoun, E.; McMurtrey III, J. E. (2000). "Estimating corn leaf chlorophyll concentration from leaf and canopy reflectance." Remote Sensing of Environment **74**(2): 229-239.

De Groot, R. S.; Wilson, M.A.; Boumans, R.M.J. (2002). "A typology for the classification, description and valuation of ecosystem functions, goods and services." Ecological Economics **41**(3): 393-408.

Di Bella, C.; Faivre, R; Ruget, F.; Seguin, B. (2005). "Using VEGETATION satellite data and the crop model STICS-Prairie to estimate pasture production at the national level in France." Physics and Chemistry of the Earth **30**(1-3 SPEC. ISS.): 3-9.

Di Bella, C. F., R. (2004). "Remote sensing capabilities to estimate pasture production in France." INT. J. REMOTE SENSING, **25**(23): 5359-5372.

Drake, JB; Dubayah, R; Clark, DB; Knox, RG; Blair, JB; Hofton, MA; Chazdon, RL; Weishempel, JF;Prince, SD. 2002. Estimation of tropical forest structural characteristics using large-footprint Lidar. *Remote Sensing of Environment* 79, 305-319.

ENVI (2003). ENVI User's Guide, Research Systems Inc.

Field, C. B.; Randerson, J. T.; Malmstrom, C. M. (1995). "Global net primary production: Combining ecology and remote sensing." Remote Sensing of Environment **51**(1): 74-88.

Foody, G. M.; Boyd, D. S.; Cutler, M. E. J. (2003). "Predictive relations of tropical forest biomass from Landsat TM data and their transferability between regions." Remote Sensing of Environment **85**(4): 463-474.

Gallo, K. P.; Daughtry, C. S. T.; Wiegand, C. L. (1993). "Errors in measuring absorbed radiation and computing crop radiation use efficiency." Agronomy Journal **85**(6): 1222-1228.

Gastellu-Etchegorry, J. P.; Gascon, F.; Esteve, P. (2003). "An interpolation procedure for generalizing a look-up table inversion method." Remote Sensing of Environment **87**(1): 55-71.

Geerling, G. K., E.; Abbing, L.; Beekers, B.; Bekhuis, J.; Havinga, H.; Helmer, W.; Mannaerts, J.; Meeuwissen, Th.; Peters, B.; Smits, A.; Snel S.; van Westreenen, B. (2005). "Floodplain Management by Cyclic Rejuvenation."

Geerling, G. W. R. A.M.J.; Leuven, R.S.E.W; van den Berg, J.H.; Breedveld, M.; Liefhebber, D.; Smits, A. (2005). Succession and rejuvenation in floodplains along the River Allier (France). Lecture notes. University of Nijmegen, The Netherlands.

Gillespie, TW; Brock, J;Wright, CW. 2004. Prospects for quantifying structure, floristic composition and species richness of tropical forests. *INT. J. REMOTE SENSING,* 25, 707-715.

Goel, N. S.; Thompson, R. L. (1984). "Inversion of vegetation canopy reflectance models for estimating agronomic variables. IV. Total inversion of the SAIL model." Remote Sensing of Environment **15**(3): 237-253.

Goel, N. S.; Thompson, R. L. (2000). "A snapshot of canopy reflectance models and a universal nodel for the radiation regime." Remote Sensing Reviews **18**(2): 197-225.

Green, A. A.; Berman, M.; Switzer, P.; Craig, M. D. (1988). "Transformation for ordering multispectral data in terms of image quality with implications for noise removal." IEEE Transactions on Geoscience and Remote Sensing **26**(1): 65-74.

Grignetti, A.; Salvatori, R.; Casacchia, R.; Manes, F. (1997). "Mediterranean vegetation analysis by multi-temporal satellite sensor data." International Journal of Remote Sensing **18**(6): 1307-1318.

Hamblin, A. (2001). Australia State of the Environment Report 2001. CSIRO. Canberra, Australia, Department of the Environment and Heritage.

Haselwimmer, C. (2005). An investigation into the factors that affect the reflectance and sensor response of leaves in the optical domain using the PROSPECT radiative transfer model. Remote Sensing – Vegetation Science.

Hooijer, A. K. F; Kwadijk, J; Pedroli, B. (2002). "Towards Sustainable Flood Risk Management in the Rhine and Meuse River Basins. Mail results of the research project." NCR **18**(1568-234X).

Huete, A. R. (1988). "A soil-adjusted vegetation index (SAVI)." Remote Sensing of Environment **25**(3): 295-309.

Huete, A. R.; Jackson, R. D.; Post, D. F. (1985). "Spectral response of a plant canopy with different soil backgrounds." Remote Sensing of Environment **17**(1): 37-53.

Hunt Jr., E. R.; Daughtry, C. S. T.; McMurtrey III, J. E.; Walthall, C. L.; Cavigelli, M. (2005). "Evaluation of digital photography from model aircraft for remote sensing of crop biomass and nitrogen status." Precision Agriculture **6**(4): 359-378.

Jacquemoud, S. (1993). "Inversion of the PROSPECT+SAIL canopy reflectance model from AVIRIS equivalent spectra: theoretical study." Remote Sensing of Environment **44**(2-3): 281-292.

Jacquemoud, S.; Bacour, C.; Poilvé, H.; Frangi, J.-P. (2000). "Comparison of four radiative transfer models to simulate plant canopies reflectance: Direct and inverse mode." Remote Sensing of Environment **74**(3): 471-481.

Jacquemoud, S.; Baret, F.; Andrieu, B.; Danson, F. M.; Jaggard, K. (1995). "Extraction of vegetation biophysical parameters by inversion of the PROSPECT+SAIL models on sugar beet canopy reflectance data. Application to TM and AVIRIS sensors." Remote Sensing of Environment **52**(3): 163-172.

Jacquemoud, S.; Baret, F. (1990). "PROSPECT: A model of Leaf Optical Properties Spectra." Remote Sensing of Environment **34**: 75-91.

Kanemasu, E. T. (1990). Estimating grassland biomass using remotely sensed data. Applications of remote sensing in agriculture**:** 185-199.

Keijzer, M.; Babovic, V.; Baptist, M.; Uthurburu, J. R. (2005). Determining equations for vegetation induced using genetic programming. GECCO 2005 - Genetic and Evolutionary Computation Conference.

Koetz, B.; Baret, F.; Poilvé, H.; Hill, J. (2005). "Use of coupled canopy structure dynamic and radiative transfer models to estimate biophysical canopy characteristics." Remote Sensing of Environment **95**(1): 115-124.

Kooistra, L., Jan Clevers, Michael Schaepman, Han van Dobben, Wieger Wamelink, Karte Sykora, Jan Hotland, Okke Batelaan, Luc Bertels, Walter Debruyn, Jan Bogaert, "the HyEco Group" (2005). "Linking biochemical and biophysical variables derived from Imaging Spectrometers to Ecological Models - The HyEco'04 Group shoot."

Kooistra L., Liras Laita E., Mengesha T., Verbeiren B., Batelaan O., van Dobben H., Schaepman M., Schaepman&Strub G. and Stuiver J. (2005). HyEco'04: an airborne imaging spectroscopy campaign in the floodplain Millingerwaard, the Netherlands. Wageningen, The Netherlands, Centrum voor GeoInformatie**:** 80.

Liras-Laita, E. (2005). Imaging Spectroscopy for Ecological Monitoring at the Test Site the Millingerwaard: Species Mapping using Spectral Libraries and Soil-Vegetation-Atmosphere-Transfer Models. Laboratory of Geo-Information Science and Remote Sensing. Wageningen, Wageningen University and Research Centre**:** 48.

Laurent, J.-M.; Bar-Hen, A.; François, L.; Ghislain, M.; Cheddadi, R. (2004). "Refining vegetation simulation models: From plant functional types to bioclimatic affinity groups of plants." Journal of Vegetation Science **15**(6): 739-746.

Lawrence, R. L.; Ripple, W. J. (1998). "Comparisons among vegetation indices and bandwise regression in a highly disturbed, heterogeneous landscape: Mount St. Helens, Washington." Remote Sensing of Environment **64**(1): 91-102.

Liang, S. (2004). Quantitative Remote Sensing of Land Surfaces, Jonh Wiley & Sons, Inc.

Lim, K. S.; Treitz, P. M. (2004). "Estimation of above ground forest biomass from airborne discrete return laser scanner data using canopy-based quantile estimators." Scandinavian Journal of Forest Research **19**(6): 558-570.

Lobell, D. B.; Asner, G. P.; Ortiz-Monasterio, J. I.; Benning, T. L. (2003). "Remote sensing of regional crop production in the Yaqui Valley, Mexico: Estimates and uncertainties." Agriculture, Ecosystems and Environment **94**(2): 205-220.

Lu, D. (2005). "Aboveground biomass estimation using Landsat TM data in the Brazilian Amazon." International Journal of Remote Sensing **26**(12): 2509-2525.

Mallinis, G; Koutsias, N; Makras, A;Karteris, M. 2004. Forest Parameters Estimation in a European Mediterranean Landscape Using Remote Sensing Data. *Forest Science* 50, 450-460.

Mengesha, T. G. (2005). Validation of ground biophysical products using Imaging Spectroscopy in a softwood forest. Laboratory of Geo-Information Science and Remote Sensing. Wageningen, The Netherlands, Wageningen University and Research Centre**:** 78.

Merrill, E. H.; Bramble-Brodahl, M. K.; Marrs, R. W.; Boyce, M. S. (1993). "Estimation of green herbaceous phytomass from Landsat MSS data in Yellowstone National Park." Journal of Range Management **46**(2): 151-157.

Mirik, M.; Norland, J. E.; Crabtree, R. L.; Biondini, M. E. (2005). "Hyperspectral one-meter-resolution remote sensing in Yellowstone National Park, Wyoming: II. Biomass." Rangeland Ecology and Management **58**(5): 459-465.

Mundt, J. T.; Glenn, N. F.; Weber, K. T.; Prather, T. S.; Lass, L. W.; Pettingill, J. (2005). "Discrimination of hoary cress and determination of its detection limits via hyperspectral image processing and accuracy assessment techniques." Remote Sensing of Environment **96**(3-4): 509-517.

Mutanga, O. (2004). Hyperspectral Remote Sensing of Tropical Grass Quality and Quantity. International Institute for Geoinformation Science and Earth Observation (ITC). Enschede (The Netherlands), Wageningen University (The Netherlands)**:** 209.

Nichol, J.; Lee, C. M. (2005). "Urban vegetation monitoring in Hong Kong using high resolution multispectral images." International Journal of Remote Sensing **26**(5): 903-918.

Ni-Meister, W.; Jupp, D. L. B.; Dubayah, R. (2001). "Modeling lidar waveforms in heterogeneous and discrete canopies." IEEE Transactions on Geoscience and Remote Sensing **39**(9): 1943-1958.

Olioso, A.; Braud, I.; Chanzy, A.; Courault, D.; Demarty, J.; Kergoat, L.; Lewan, E. Ottlé, C.; Prévot, L.; Zhao, W. G.; Calvet, J.-C.; Cayrol, P.; Jongschaap, R.; Moulin, S.; Noilhan, J.; Wigneron, J.-P. (2002). "SVAT modeling over the Alpilles-ReSeDA experiment: Comparing SVAT models over wheat fields." Agronomie **22**(6): 651-668.

Paruelo, J. M.; Lauenroth, W. K. (1996). "Relative abundance of plant functional types in grasslands and shrublands of north America." Ecological Applications **6**(4): 1212-1224.

Paruelo, J. M.; Lauenroth, W. K.; Roset, P. A. (2000). "Estimating aboveground plant biomass using a photographic technique." Journal of Range Management **53**(2): 190-193.

Paruelo, J. M.; Oesterheld, M.; Di Bella, C. M.; Arzadum, M.; Lafontaine, J.; Cahuepé, M.; Rebella, C. M. (2000). "Estimation of primary production of

subhumid rangelands from remote sensing data." Applied Vegetation Science **3**(2): 189-195.

Prevot, L.; Baret, F.; Chanzy, A.; Olioso, A.; Wigneron, J. P.; Autret, H.; Baudin, F.; Bessemoulin, P.; Bethenod, O.; Blamont, D.; Blavoux, B.; Bonnefond, J. M.; Boubkraoui, S.; Bouman, B. A. M.; Braud, I. (1998). Assimilation of multi-sensor and multi-temporal remote sensing data to monitor vegetation and soil: the Alpilles-ReSeDA project. International Geoscience and Remote Sensing Symposium (IGARSS).

Rademacher, JGM;Wolfert, HP. 1994. Het Rivier-Ecotopen-Stelsel: een indeling van ecologisch relevante ruimtelijke eenheden ten behoeve van ontwerp -en beleids studies in het buitendijkse rivierengebied. Lelystad: Rijswaterstaat.

Rahman, M. M.; Csaplovics, E.; Koch, B. (2005). "An efficient regression strategy for extracting forest biomass information from satellite sensor data." International Journal of Remote Sensing **26**(7): 1511-1519.

Reeves, M. C.; Zhao, M.; Running, S. W. (2006). "Applying improved estimates of MODIS productivity to characterize grassland vegetation dynamics." Rangeland Ecology and Management **59**(1): 1-10.

Rouse, J. (1974). Monitoring the Vernal Advancement and Retrogradation (greenwave Effect) of Natural Vegetation.

Ruimy, A.; Kergoat, L.; Bondeau, A. (1999). "Comparing global models of terrestrial net primary productivity (NPP): Analysis of differences in light absorption and light-use efficiency." Global Change Biology **5**(SUPPL. 1): 56-64.

Samimi, C.; Kraus, T. (2004). "Biomass estimation using Landsat-TM and -ETM+. Towards a regional model for Southern Africa?" GeoJournal **59**(3): 177-187.

Schino, G.; Borfecchia, F.; De Cecco, L.; Dibari, C.; Iannetta, M.; Martini, S.; Pedrotti, F. (2003). "Satellite estimate of grass biomass in a mountainous range in central Italy." Agroforestry Systems **59**(2): 157-162.

Schlerf, M.; Hill, J.; Atzberger, C. (2005). "Remote sensing of forest biophysical variables using HyMap imaging spectrometer data." Remote Sensing of Environment **95**(2): 177-194.

Schmidt, A.; van Dobben, H.; Wamelink, W.; Kooistra, L.; Schaepman, M. (2005). HYECO'04: Using hyperspectral reflectance data to initialise ecological models. 4th Workshop on Imaging Spectroscopy, Warsaw, EARSeL.

SDF, I. (2003). Sustainable development of floodplains. Arnhem, SDF**:** 24.

Shoshany, M. (2000). "Satellite remote sensing of natural Mediterranean vegetation: A review within an ecological context." Progress in Physical Geography **24**(2): 153-178.

Smith, M. O.; Ustin, S. L.; Adams, J. B.; Gillespie, A. R. (1990). "Vegetation in deserts: I. A regional measure of abundance from multispectral images." Remote Sensing of Environment **31**(1): 1-26.

Steinmetz, S.; Guerif, M.; Delecolle, R.; Baret, F. (1990). "Spectral estimates of the absorbed photosynthetically active radiation and light-use efficiency of a winter wheat crop subjected to nitrogen and water deficiencies." INT. J. REMOTE SENSING, **11**: 1797– 1808.

Su, H.; Ransom, M. D.; Kanemasu, E. T. (1997). "Simulating wheat crop residue reflectance with the SAIL model." International Journal of Remote Sensing **18**(10): 2261-2267.

Thenkabail, P. S. (2003). "Biophysical and yield information for precision farming from near-real-time and historical Landsat TM images." International Journal of Remote Sensing **24**(14): 2879-2904.

Thenkabail, P. S.; Smith, R. B.; De Pauw, E. (2000). "Hyperspectral vegetation indices and their relationships with agricultural crop characteristics." Remote Sensing of Environment **71**(2): 158-182.

Todd, S. W.; Hoffer, R. M.; Milchunas, D. G. (1998). "Biomass estimation on grazed and ungrazed rangelands using spectral indices." International Journal of Remote Sensing **19**(3): 427-438.

Trémolieres, M.; Schmitt, D.; Sánchez-Pérez, J. M.; Schnitzler, A. (1998). "Impact of river management history on the community structure, species composition and nutrient status in the Rhine alluvial hardwood forest." Plant Ecology **135**(1): 59-78.

van den Bosch, L. (2003). Influence of vegetation on flow and morphology in the river Allier, France. Civil Engineering and Geosciences. Delft, The Netherlands, Delft University of Technology**:** 119.

Verhoef, W. (1984). "Light scattering by leaf layers with application to canopy reflectance modeling: the SAIL model." Remote Sensing of Environment **16**(2): 125-141.

Weiss, M.; Baret, F.; Myneni, R. B.; Pragnere, A.; Knyazikhin, Y. (2000). "Investigation of a model inversion technique to estimate canopy biophysical variables from spectral and directional reflectance data." Agronomie **20**(1): 3-22.

Williams, A. P.; Hunt Jr., E. R. (2002). "Estimation of leafy spurge cover from hyperspectral imagery using mixture tuned matched filtering." Remote Sensing of Environment **82**(2-3): 446-456.

Wylie, B. K.; Meyer, D. J.; Tieszen; Mannel, S. (2002). "Satellite mapping of surface biophysical parameters at the biome scale over the North American grasslands a case study." Remote Sensing of Environment **79**(2-3): 266-278.

Zagajewski, B. S.; Wrzesien, M. (2004). "Hyperspectral remote sensing techniques for mountains vegetation investigation." Przeglad Geofizyczny **49**(3-4): 115-129.

Zheng, D.; Chen, J.; Bresee, M.; Ryu, S.-R.; Rademacher, J.; Crow, T.; Le Moine, J. (2004). "Estimating aboveground biomass using Landsat 7 ETM+ data across a managed landscape in northern Wisconsin, USA." Remote Sensing of Environment **93**(3): 402-411.

Web References:

Web 1: Freude am fluss Program

http://www.ru.nl/aspx/get.aspx?xdl=/views/run/xdl/page&SitIdt=289&VarIdt=412&ItmIdt=31385

Web 2: Modelling vegetation succession in floodplains

http://www.wldelft.nl/rnd/intro/topic/modelling-of-veg

APPENDIXES

APPENDIX 1: GENERAL INFORMATION

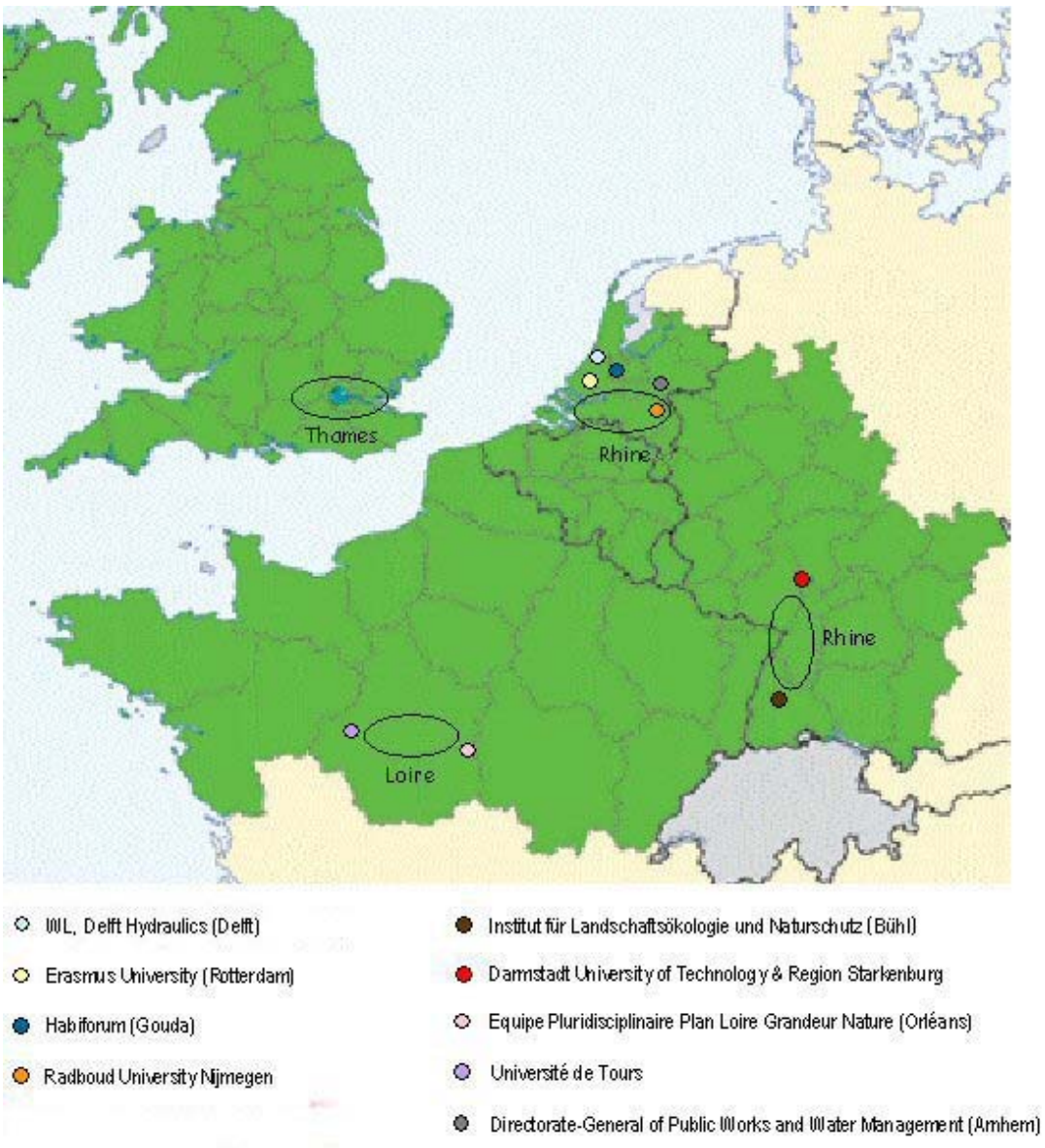

Figure 25. .. Map of the area affected by the project *Freude am Fluss*

APPENDIX 2. FIELD WORK

Table 20. Height, coverage and dominant species per sampling plot

Samples	Height (cm)	Most common specie	Coverage (%)	PFT
2	2-4	Trifolium repens	100	Grazed-Grasslands
3	110-120	Rubus caesius	100	Mixed Herbs
4	130	Rubus caesius	100	Mixed Herbs
5	3-20	Poa annua	100	Grazed-Grasslands
6	100	Rubus caesius	95	Mixed Herbs
7	120	Lythrum salycaria	100	Mixed Herbs
8	100	Epilobium tetragonum	95	Mixed Herbs
9		Rubus caesius	100	Mixed Herbs
10	100	Calamagrostis epigejos	100	Mixed Herbs
11	80	Rubus caesius	100	Mixed Herbs
12	130	Rubus caesius	100	Mixed Herbs
13	5	Potentilla reptans	95	Grazed-Grasslands
14	35	Potentilla reptans	90	Grazed-Grasslands
15		Cynodon dactylon	100	Grazed-Grasslands
16	80	Cirsium arvense	15	Mixed Herbs
17		Calamagrostis epigejos	70	Mixed Herbs
18	30-60	Saponaria officinalis	30	Mixed Herbs
19	35	Festuca rubra	80	Grazed-Grasslands
20		Calamagrostis epigejos	90	Mixed Herbs
21	10	Trifolium repens	95	Grazed-Grasslands
22	100	Urtica dioica	80	Mixed Herbs

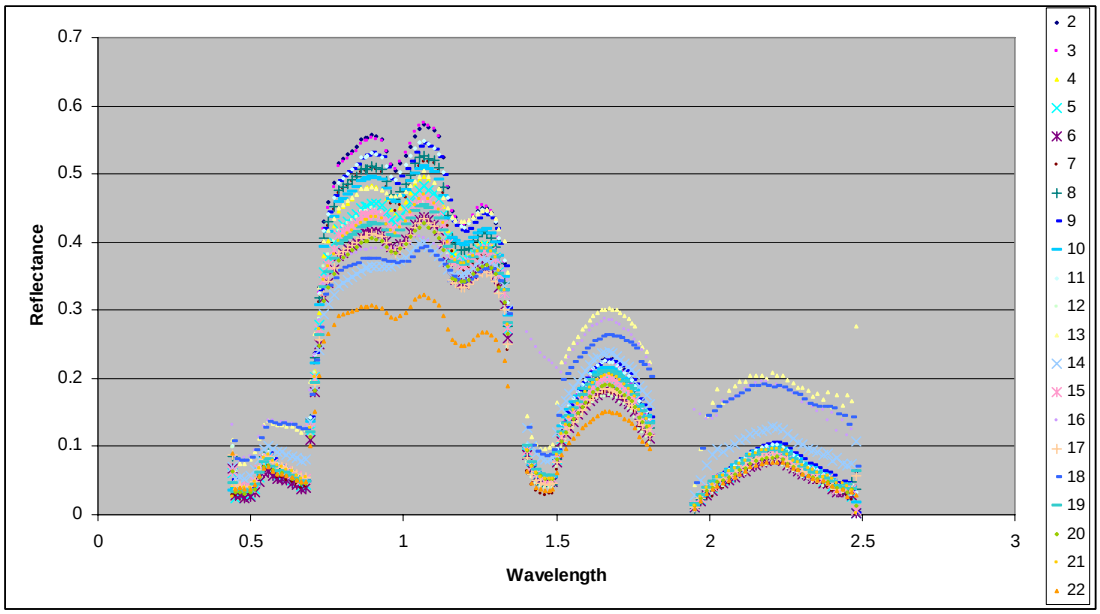

Figure 26. .. Spectral curves of the 21 sample plots

Appendix 2: Field work

Table 21. Sample coordinates and the pixel centre in which they are located. The highlighted numbers show the differences higher than 2 metres in the Northing and Easting coordinates values. The last column corresponds to the total distance between sampling and pixel centres.

plot nr	Field samples coordinates		Pixel location		Deviation		Centres deviation
	Northing (N)	Easting (E)	Northing (N)	Easting (E)	N deviation	E deviation	
2	5750403.686	706161.885	5750402.5	706162.5004	1.186	-0.6154	1.336156113
3	5750405.912	706149.765	5750407.5	706147.5004	-1.588	2.2646	2.765891748
4	5750447.425	706129.26	5750447.5	706127.5004	-0.075	1.7596	1.761197649
5	5750453.35	706151.535	5750452.5	706152.5004	0.85	-0.9654	1.286272584
6	5750543.614	706194.569	5750542.5	706192.5004	1.114	2.0686	2.349489723
7	5750559.715	706235.616	5750557.5	706237.5004	2.215	-1.8844	2.908124543
8	5750583.878	706230.492	5750582.5	706232.5004	1.378	-2.0084	2.435683592
9	5750685.955	706178.455	5750687.5	706177.5004	-1.545	0.9546	1.816118432
10	5750836.457	706090.153	5750837.5	706092.5004	-1.043	-2.3474	2.568683663
11	5750851.326	706112.493	5750852.5	706112.5004	-1.174	-0.0074	1.174023321
12	5750990.334	706080.374	5750992.5	706082.5004	-2.166	-2.1264	3.03531431
13	5751016.619	706027.505	5751017.5	706027.5004	-0.881	0.0046	0.881012009
14	5750813.683	705962.661	5750812.5	705962.5004	1.183	0.1606	1.193851482
15	5750732.783	705967.92	5750732.5	705967.5004	0.283	0.4196	0.506115757
16	5750591.248	705833.25	5750592.5	705832.5004	-1.252	0.7496	1.459247807
17	5750550.535	705843.106	5750552.5	705842.5004	-1.965	0.6056	2.056204357
18	5750475.527	705818.08	5750477.5	705817.5004	-1.973	0.5796	2.056371844
19	5750485.242	705891.859	5750487.5	705892.5004	-2.258	-0.6414	2.347329964
20	5750504.121	705919.147	5750502.5	705917.5004	1.621	1.6466	2.310613027
21	5750310.889	705867.027	5750312.5	705867.5004	-1.611	-0.4734	1.67911541
22	5750110.272	705705.724	5750112.5	705707.5004	-2.228	-1.7764	2.849487842

APPENDIX 3. VEGETATION INDICES

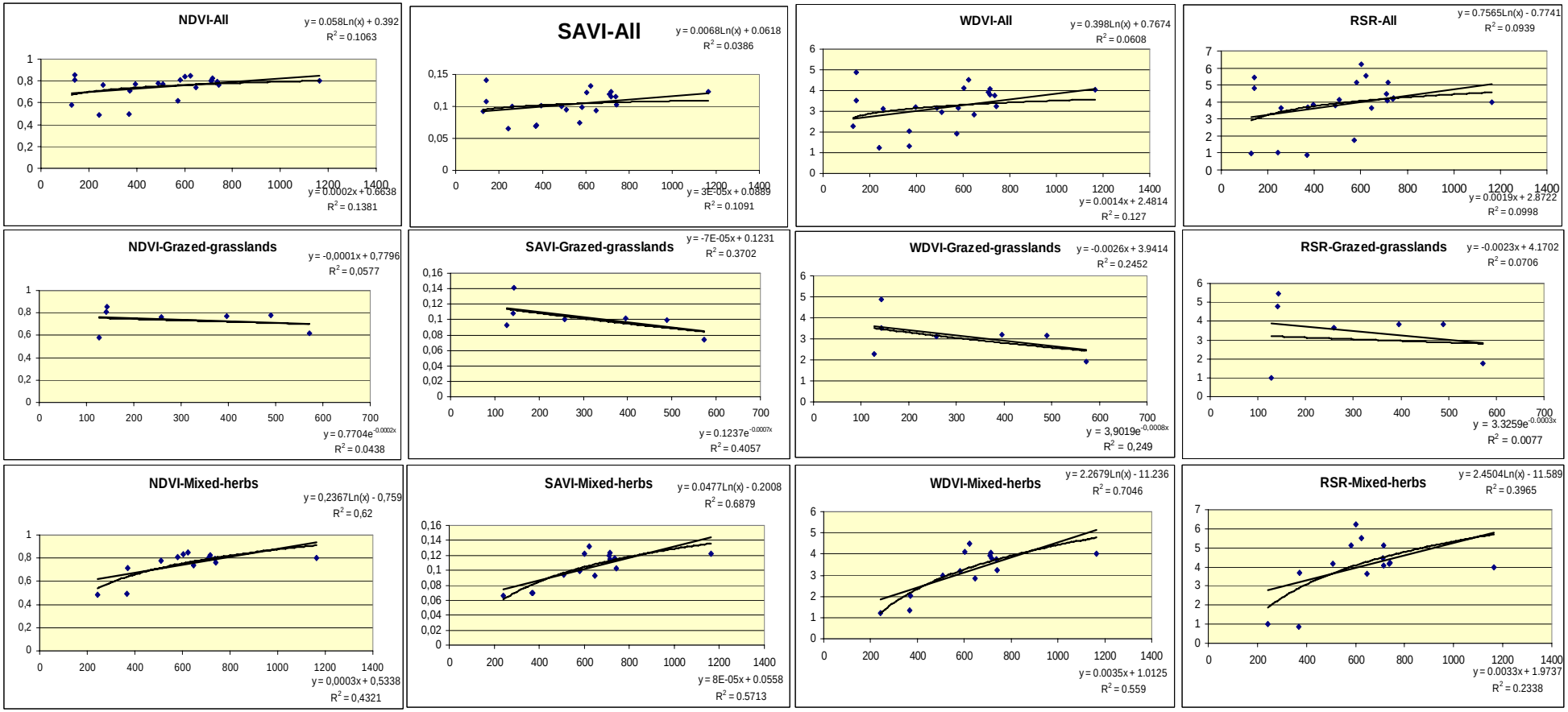

Figure 27....Relationship VI-Biomass per PFT

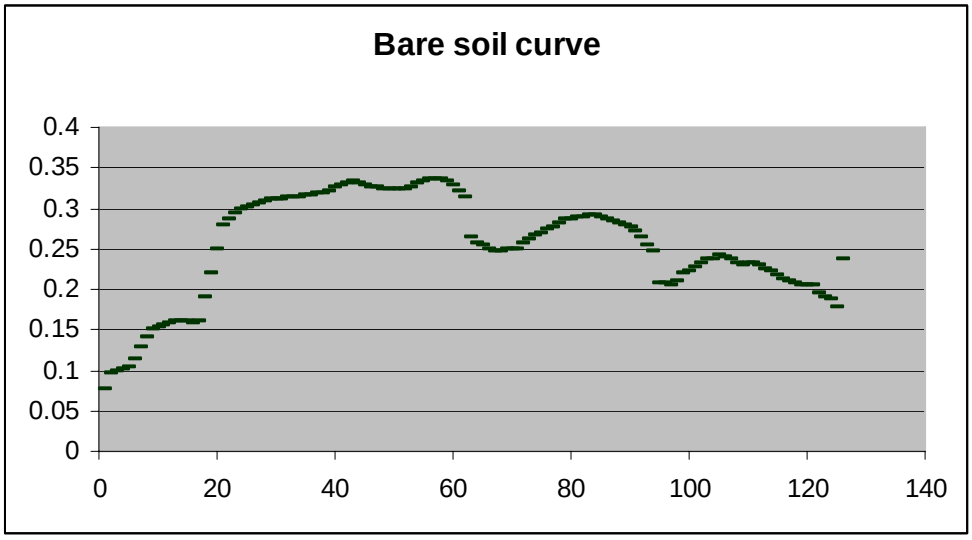

Figure 28. .. Spectrum of the bare soil considered to calculate the a parameter for WDVI.

Table 22. Comparison between estimated biomass with statistical methods and measured biomass in the field.

Grazed-grasslands		
Plot#	Field	Estimated
2	**142.88**	1485.29
5	**142.08**	601.1284
13	**127.32**	1949.868
14	**572.44**	479.787
15	**395.96**	516.6091
19	**489.64**	379.7194
21	**258.68**	760.2605

Mixed-herbs		
Plot#	Field	Estimated
3	**623.08**	1361.92
4	**715.68**	984.3438
6	**580.8**	589.7888
7	**602.36**	1128.922
8	**709.72**	1083.408
9	**714.48**	1332.929
10	**736.56**	1126.22
11	**1164.64**	1200.339
12	**741.24**	645.891
16	**368.24**	340.5791
17	**646.08**	444.8405
18	**241.88**	1676.441
20	**508.52**	303.2381
22	**371**	546.3275

APPENDIX 4: MODEL INVERSION

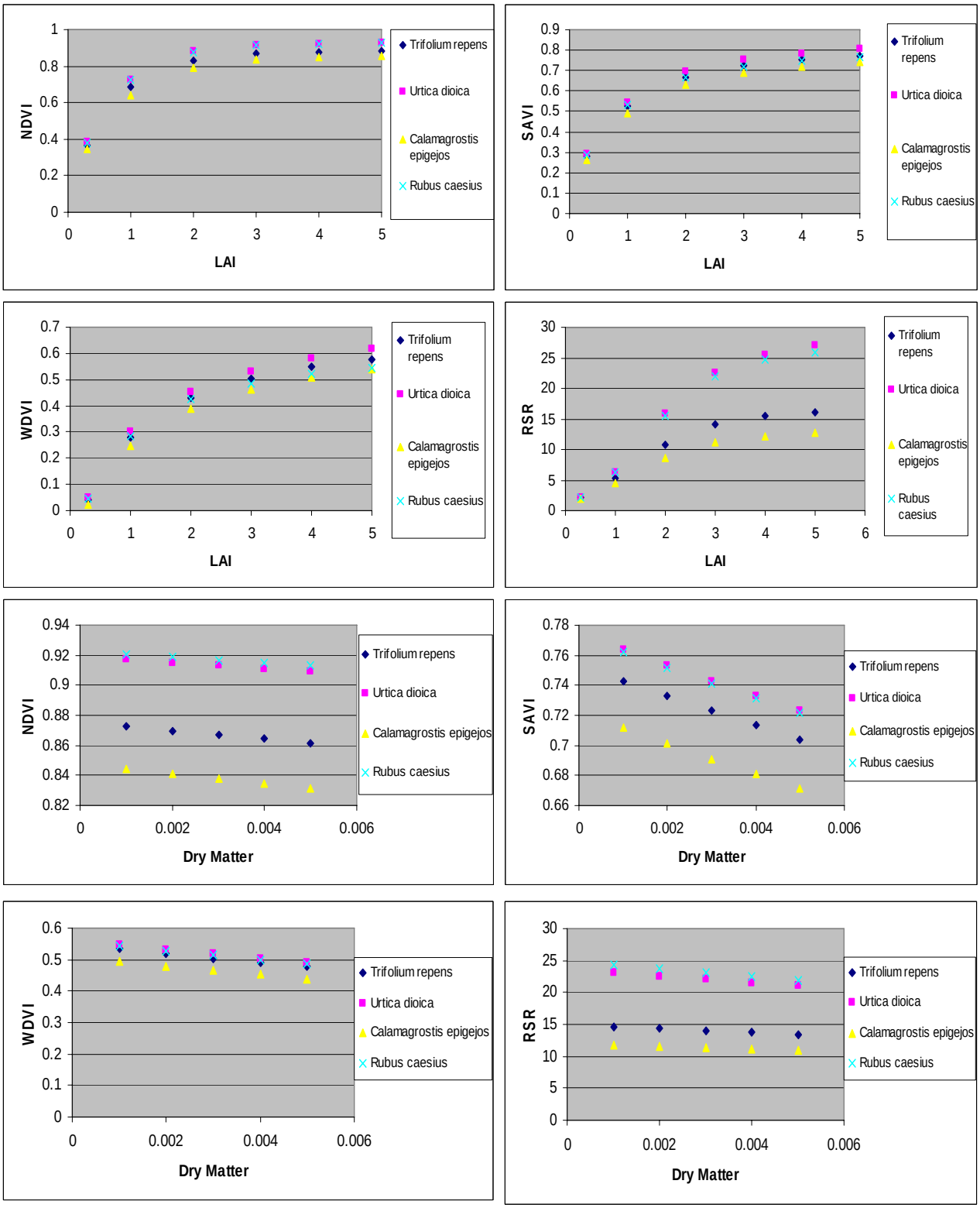

Figure 29. .. Influence of Dry matter content and LAI in the vegetation indices.

Table 23. Radiative transfer models inversion results for grazed-grasslands plots. RMSE: Root Mean Square Error, Cm: Dry matter content in the leaves, LAI: Leaf area index. The values in bold represent the lowest RMSE achieved per plot.

Sample plots		2	3	4	5	6	7	8	9	10	11
Trifolium repens	RMSE	0.090774	0.089281	0.09008	0.091942	0.09633	0.084267	0.087649	0.08908	0.089776	0.088694
	Cm	0.005	0.005	0.005	0.005	0.005	0.005	0.005	0.005	0.005	0.005
	LAI	3	3	2	2	2	3	3	3	2	3
Calamagrostis epigejos	RMSE	0.090809	0.08946	0.08889	0.091916	0.094441	0.083201	0.086354	0.088862	0.087771	0.088459
	Cm	0.005	0.005	0.005	0.005	0.005	0.005	0.005	0.005	0.005	0.005
	LAI	4	4	3	2	2	3	3	3	3	3
Urtica dioica	RMSE	0.090805	0.089245	0.088922	0.091584	0.093806	0.08315	0.087788	0.089889	0.089064	0.089745
	Cm	0.005	0.005	0.005	0.005	0.005	0.005	0.005	0.005	0.005	0.005
	LAI	4	4	3	2	2	3	3	3	3	3
Rubus caesius	RMSE	**0.086338**	**0.084667**	**0.078881**	**0.080772**	**0.080225**	**0.07319**	**0.080686**	**0.08493**	**0.081367**	**0.084884**
	Cm	0.006	0.006	0.007	0.007	0.007	0.007	0.007	0.007	0.007	0.007
	LAI	5	5	3	3	2	4	4	4	3	4

Table 24. Radiative transfer models results for mixed-herbs plots. RMSE: Root Mean Square Error, Cm: Dry matter content in the leaves, LAI: Leaf area index. The values in bold represent the lowest RMSE achieved per plot.

Sample plots		3	4	6	7	8	9	10	11	12	16	17	18	20	22
Trifolium repens	RMSE	0.089281	0.09008	0.09633	0.084267	0.087649	0.08908	0.089776	0.088694	0.089437	0.108623	0.097058	0.117384	0.099795	0.129294
	Cm	0.005	0.005	0.005	0.005	0.005	0.005	0.005	0.005	0.005	0.005	0.005	0.005	0.005	0.005
	LAI	3	2	2	3	3	3	2	3	2	1	2	1	2	2
Calamagrostis epigejos	RMSE	0.08946	0.08889	0.094441	0.083201	0.086354	0.088862	0.087771	0.088459	0.088266	**0.106354**	0.094329	0.116913	0.097085	0.123582
	Cm	0.005	0.005	0.005	0.005	0.005	0.005	0.005	0.005	0.005	0.005	0.005	0.005	0.005	0.005
	LAI	4	3	2	3	3	3	3	3	2	1	2	2	2	2
Urtica dioica	RMSE	0.089245	0.088922	0.093806	0.08315	0.087788	0.089889	0.089064	0.089745	0.089675	0.109768	0.095919	0.120704	0.097485	0.124947
	Cm	0.005	0.005	0.005	0.005	0.005	0.005	0.005	0.005	0.005	0.005	0.005	0.005	0.005	0.005
	LAI	4	3	2	3	3	3	3	3	2	1	2	1	2	2
Rubus caesius	RMSE	**0.084667**	**0.078881**	**0.080225**	**0.07319**	**0.080686**	**0.08493**	**0.081367**	**0.084884**	**0.076813**	0.108315	**0.082712**	**0.113236**	**0.084145**	**0.108294**
	Cm	0.006	0.007	0.007	0.007	0.007	0.007	0.007	0.007	0.007	0.007	0.007	0.007	0.007	0.007
	LAI	5	3	2	4	4	4	3	4	3	1	2	1	2	2